Am J Physiol Regul Integr Comp Physiol 325: R504–R522, 2023.
First published August 21, 2023; doi:10.1152/ajpregu.00165.2023

american physiological society

AMERICAN JOURNAL OF PHYSIOLOGY
REGULATORY, INTEGRATIVE AND COMPARATIVE PHYSIOLOGY

RESEARCH ARTICLE

Effects of cortisol, epinephrine, and bisphenol contaminants on the transcriptional landscape of marine mammal blubber

Lauren Kashiwabara,[1]* Laura Pirard,[2] Cathy Debier,[2] Daniel Crocker,[3] and Jane Khudyakov[1]*

[1]*Department of Biological Sciences, University of the Pacific, Stockton, California, United States;* [2]*Louvain Institute of Biomolecular Science and Technology, Université Catholique de Louvain, Louvain-la Neuve, Belgium; and* [3]*Department of Biology, Sonoma State University, Rohnert Park, California, United States*

Abstract

Top ocean predators such as marine mammals are threatened by intensifying anthropogenic activity, and understanding the combined effects of multiple stressors on their physiology is critical for conservation efforts. We investigated potential interactions between stress hormones and bisphenol contaminants in a model marine mammal, the northern elephant seal (NES). We exposed precision-cut adipose tissue slices (PCATS) from blubber of weaned NES pups to cortisol (CORT), epinephrine (EPI), bisphenol A (BPA), bisphenol S (BPS), or their combinations (CORT-EPI, BPA-EPI, and BPS-EPI) ex vivo and identified hundreds of genes that were differentially regulated in response to these treatments. CORT altered expression of genes associated with lipolysis and adipogenesis, whereas EPI and CORT-EPI-regulated genes were associated with responses to hormones, lipid and protein turnover, immune function, and transcriptional and epigenetic regulation of gene expression, suggesting that EPI has wide-ranging and prolonged impacts on the transcriptional landscape and function of blubber. Bisphenol treatments alone had a weak impact on gene expression compared with stress hormones. However, the combination of EPI with bisphenols altered expression of genes associated with inflammation, cell stress, DNA damage, regulation of nuclear hormone receptor activity, cell cycle, mitochondrial function, primary ciliogenesis, and lipid metabolism in blubber. Our results suggest that CORT, EPI, bisphenols, and their combinations impact cellular, immune, and metabolic homeostasis in marine mammal blubber, which may affect the ability of marine mammals to sustain prolonged fasting during reproduction and migration, renew tissues, and mount appropriate responses to immune challenges and additional stressors.

bisphenol; blubber; cortisol; epinephrine

INTRODUCTION

Marine mammals are top ocean predators that serve as key indicators of marine ecosystem health and stability. Many marine mammal populations are in decline and are vulnerable to the increasing and intensifying stressors caused by anthropogenic activity, with up to 25% of marine mammal species currently listed as threatened (1, 2). Anthropogenic stressors include prey depletion, habitat degradation, and physical, chemical, and sound pollution, among many others (1, 3). Anthropogenic disturbance may induce physiological stress responses in marine mammals, which are mediated by two systems: the sympathetic nervous system and sympathetic adrenal medulla (SAM), which produce catecholamines (i.e., norepinephrine and epinephrine), and the hypothalamic-pituitary-adrenal (HPA) axis and glucocorticoid (GC) hormones (e.g., cortisol) produced by the adrenal cortex. Both systems mobilize energy stores, e.g., by stimulating lipolysis in adipose tissue, to provide substrates for the increased energy expenditure of behavioral and physiological responses to stress (4). If experienced repeatedly or chronically, stress may deplete energy stores and impact the ability of animals to respond to additional stressors, mount immune and antioxidant responses, or engage in energy-intensive life history stages such as postnatal development and reproduction (5–8).

Catecholamines mainly exert their effects on target tissues via rapid, nongenomic signaling by adrenergic receptors. For example, in adipose tissue, activation of β-adrenergic receptor, a type of G protein-coupled receptor (GPCR), leads to phosphorylation and activation of enzymes and their regulators involved in lipolysis and thermogenesis, which is mediated by protein kinase A (PKA) and its allosteric activator cAMP (9, 10). However, downstream effectors of adrenergic signaling also include transcription factors such as cAMP response element-binding protein (CREB) and CREB-regulated transcriptional coactivators (CRTCs), which alter gene expression in response to catecholamines (11, 12). GCs, in contrast, mainly exert their effects via genomic mechanisms by binding to intracellular receptors (glucocorticoid receptors, GR) and altering gene expression. In adipose tissue, GR

*L. Kashiwabara and J. Khudyakov contributed equally to this work.
Correspondence: J. Khudyakov (jkhudyakov@pacific.edu).
Submitted 2 July 2023 / Revised 4 August 2023 / Accepted 16 August 2023

target genes include those involved in lipolysis and adipocyte maturation, or adipogenesis (10, 13). GCs also have nongenomic effects that are, in part, mediated by cAMP (14). Because of the transient nature of the SAM response, catecholamines have been mostly overlooked in studies of stress in wildlife, which have focused on GC measurements, thereby missing part of the stress response (4). However, repeated or chronic stress has the potential to facilitate downstream interactions between the two signaling pathways. Recent studies have shown that in liver, CREB, and GR facilitate each other's loading on enhancers of shared target genes, either directly or indirectly via coactivators such as CRTC2 and PGC1A (15–17). While we have previously identified genes in marine mammal blubber that are responsive to experimental HPA axis stimulation, these studies were conducted under anesthesia, which blunts the SAM response to research handling (18–20). The impacts of catecholamines and their interactions with GCs on gene expression in marine mammals, and most wild animals, remain unknown.

Marine mammals are increasingly exposed to multiple, simultaneous stressors (e.g., physical disturbance and chemical pollution), and understanding their combined effects on physiology and health is critical for conservation efforts (21). The physiological effects of stress hormones may be modulated by endocrine-disrupting chemicals (EDCs) of anthropogenic origin, many of which are increasing in prevalence in marine ecosystems due to coastal runoff and breakdown of microplastics (22). Pervasive EDCs include bisphenol A (BPA) and its alternatives (e.g., bisphenol S, BPS), which are additives/monomers used in commercial plastics manufacturing that have been detected in marine mammals (23). While these contaminants do not persist in animal tissues, ingestion of prey contaminated with bisphenols may result in chronic exposure, which may alter cortisol, testosterone, and thyroid hormone levels, as has been shown in several cetacean species (24). In humans and rodents, bisphenols have been associated with obesity and insulin resistance, potentially via their interaction with nuclear hormone receptors, including estrogen receptors, estrogen-related receptors, androgen receptor, peroxisome proliferator-activated receptors (PPARs), thyroid hormone receptors, and GR (25). In adipocytes, bisphenols have been shown to stimulate lipogenesis, adipogenesis, interfere with insulin signaling and adipokine production, and contribute to oxidative stress (26, 27). Therefore, bisphenol exposure has the potential to alter metabolic homeostasis and adaptive responses to other stressors in marine mammals.

We decided to investigate the downstream effects of and potential interactions between stress hormones and bisphenol contaminants in a model marine mammal, the northern elephant seal (NES, *Mirounga angustirostris*). The NES is a deep-diving, pelagic species that fasts on land for up to 3 mo during postnatal development, annual molting, and reproduction, at which times animals are easily accessible for research handling. Although it is challenging to accurately measure bisphenol levels in fasting animals, BPA has been detected in myctophid fishes of the North Pacific (mean BPA concentrations 0.686–1.28 ng/sample wet weight), a major prey source of NES, which feed on mesopelagic fish 1,000–2,000 times per day during foraging trips lasting up to 10 mo (28–30). Therefore, it is likely that NES are routinely exposed to bisphenols via their diet (potentially consuming ~2 μg BPA/day). Using our previously developed ex vivo culture system of precision-cut adipose tissue slices, or PCATS (31), we exposed NES blubber to biologically relevant concentrations of cortisol, epinephrine, and BPA and BPS and their combinations and determined their effects on the transcriptome as a readout of downstream effects on blubber physiology. We identified genes that were differentially regulated in response to each treatment as well as core groups of genes that responded to multiple treatments, providing novel information on interactive impacts of multiple stressors in marine mammals.

METHODS

Sample Collection

All animal handling procedures were conducted under National Marine Fisheries Service permit 23188 and were approved by the Sonoma State University Institutional Animal Care and Use Committee. Blubber samples were collected in Spring 2019 from weaned NES pups ($n = 3$; females) early in their postweaning fasting period (as determined by presence of natal pelage) at Año Nuevo State Reserve (San Mateo County, CA), as described previously (31). Animals were chemically immobilized using an intramuscular injection of 1 mg/kg tiletamine-zolazepam HCl (Telazol, Fort Dodge Animal Health); sedation was maintained with intravenous doses of 0.25–1 mg/kg ketamine as needed (Ketaset, Fort Dodge Animal Health). Blubber biopsies were collected from the posterior flank of each animal using a 6.0-mm diameter biopsy punch (Miltex Integra). Samples were rinsed in phosphate-buffered saline (PBS, Life Technologies) and stored until return to the laboratory in oxygenated sampling medium composed of Dulbecco's modified Eagle's medium (DMEM) with 4.5 g/L glucose, 10 mM HEPES, 2 mM Glutamax (Life Technologies), and antibiotic and antifungal mixture [100 U/mL penicillin, 100 U/mL streptomycin, 250 ng/mL amphotericin, 1 mg/mL gentamycin (Life Technologies), and 40 U/mL nystatin (Sigma-Aldrich)] at ~25°C, as previously described (31).

Culture Experiments

Blubber tissue was processed within 2–4 h after collection as described previously (31). Biopsies were dissected into three portions (innermost, middle, and outermost), and each portion was precision cut into 1-mm PCATS using a mouse and rat spinal cord matrix device (Ted Pella, Inc.) and razor blades. PCATS were weighed, and four slices were added to each well of a 24-well plate with 1 mL of prewarmed sterile culture medium [DMEM with 1 g/L glucose (Gibco) supplemented with 5% fetal bovine serum (FBS; Gibco), 2% (wt:vol) bovine serum albumin fraction V (Research Products International), and an antibiotic-antimycotic mixture (100 U/mL penicillin, 100 U/mL streptomycin, 250 ng/mL amphotericin, 50 μg/mL gentamicin, and 40 U/mL nystatin)]. PCATS derived from inner, middle, and outer blubber were cultured separately in separate wells to distinguish metabolic responses of each layer to hormones and contaminants for a different study. Plates were placed in an incubator (37°C, 5% of CO_2) on a shaker for 3 h; media was replaced after 3 h of incubation to remove cell debris resulting from slicing, and PCATS were cultured for an additional 48 h (Fig. 1).

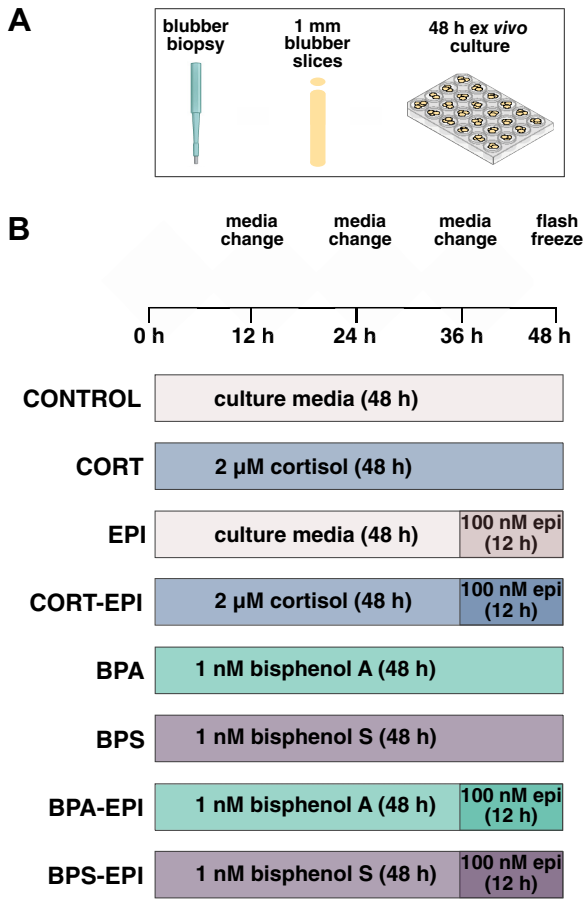

Figure 1. Experimental design of the study. *A*: blubber biopsies were obtained from free-ranging weaned elephant seal pups ($n = 3$), precision-cut into 1-mm slices (precision-cut adipose tissue slices, PCATS), and cultured in multiwell plates for 48 h. PCATS were cultured in control media (gray) or with the addition of cortisol (blue, added during entire 48-h duration of culture), epinephrine (shaded, added during last 12 h of culture only), bisphenol A (BPA, teal, for 48 h), bisphenol S (BPS, purple, for 48 h), and their combinations as shown in *B*. Media was replaced every 12 h, and PCATS were flash-frozen for RNA extraction after 48 h of treatment. CORT, cortisol; EPI, epinephrine.

PCATS were exposed to the following treatments (Fig. 1): control (culture media for 48 h); 2 μM cortisol (CORT, Sigma-Aldrich) for 48 h; 100 nM epinephrine (EPI, epinephrine bitartrate salt, Sigma-Aldrich) added for last 12 h of culture, after 36 h of culture in control media; 2 μM cortisol for 48 h with 100 nM epinephrine (CORT-EPI) added for the last 12 h of culture, 1 nM bisphenol A (BPA, Sigma-Aldrich) for 48 h; 1 nM bisphenol S (BPS, Sigma-Aldrich) for 48 h; 1 nM BPA for 48 h with 100 nM epinephrine (BPA-EPI) added for the last 12 h; and 1 nM BPS for 48 h with 100 nM epinephrine (BPS-EPI) added for the last 12 h. Cortisol and epinephrine treatment concentrations were determined based on levels reported in vivo and those found sufficient to induce a lipolytic response in PCATS from NES, respectively (20). BPA and BPS treatment concentrations were determined based on the range of phenol derivative concentrations that were measured in the blood of Baltic gray seals (*Halichoerus grypus*) (32) and that were shown to induce significant effects on lipolysis in 3T3-L1 mouse adipocytes (33). After 48 h of each treatment, PCATS were rinsed in PBS, flash-frozen in RNase-free 2.0-mL bead tubes with 2.8-mm stainless steel beads (VWR), and stored at −80°C until further processing. PCATS derived from inner, middle, and outer blubber were pooled to obtain sufficient tissue mass (~60 mg) for RNA isolation.

RNA Isolation and Sequencing

Frozen PCATS were homogenized in 1 mL of Qiazol (Qiagen) in a Bullet Blender Storm 24 instrument (Next Advance) for two cycles of 2 min at power 12, followed by shearing with a 21-gauge needle. Total RNA was isolated using the RNeasy Lipid Mini Kit (Qiagen) with a 15-min on-column DNase I digest. RNA quantity was estimated using the RNA High Sensitivity Assay on the Qubit 3.0 fluorometer (Life Technologies). RNA integrity was assessed using the RNA 6000 Pico Assay on the 2100 Bioanalyzer (Agilent Technologies). The mean (± SD) RNA integrity number (RIN) for all samples was 8.7 ± 0.3. Strand-specific low-input (200 ng) cDNA library preparation and Illumina paired-end 150-bp sequencing were conducted by Novogene Corporation, Inc. (Beijing, China).

Transcriptome Analysis

Transcriptome analyses were conducted using the Bridges 2 high-performance computing cluster at the Pittsburgh Supercomputing Center using Extreme Science and Engineering Discovery Environment (XSEDE; allocation TG-IBN150010) (34). Raw sequencing files are available at NCBI Short Read Archive (Accession No.: PRJNA989379). Sequence quality was assessed using FastQC v0.11.3. The transcriptome was assembled de novo using Trinity v2.11.0 (35). The completeness of the transcriptome assembly was assessed using BUSCO v5.0.0 and the *Mammalia* database (36). Transcripts were annotated by BLASTX against the UniProt SwissProt database (downloaded on March 8, 2021) using DIAMOND v2.0.7 in ultrasensitive mode with an *e*-value threshold of 1*e*-3 (37). The transcriptome assembly and annotation files are available at https://doi.org/10.6084/m9.figshare.21804192. Transcript abundance was estimated using kallisto v0.46.1 in alignment-free mode (38).

Statistical Analyses

All statistical analyses and visualizations were conducted using R (v4.1.0) and R-studio (v1.4.1106) (39). Supplemental files and figures are accessible at https://doi.org/10.6084/m9.figshare.23612637.v3. Differential gene expression analyses were conducted using "tximport" and DESeq2 v1.35.0 (40), with blocking by study subject from which blubber biopsies for PCATS were obtained (design = ~ subject + treatment). Differentially expressed genes (DEG) were extracted using the DESeq2 results function ($\alpha = 0.1$, pAdjustMethod = "BH"). DEG lists were filtered to remove genes with log2 fold change < |1| and those lacking annotation. All DEG data are available in Supplemental File S1. Potential interactive effects of hormone and bisphenol treatments on gene expression were examined by coding CORT, EPI, BPA, and BPS treatments as separate factors and rerunning DESeq2 with an interaction term (e.g., design = ~ subject + CORT + EPI + CORT:EPI). Genes with log2 fold change > 0 and < 0 (at *P*.adj < 0.1) were considered synergistically and antagonistically regulated, respectively (41). Overlaps between DEG sets were analyzed using

"UpSetR" package (42) and GeneVenn (http://www.bioinformatics.org/gvenn/). Overrepresentation analyses of DEG were conducted using "clusterProfiler" package against the human genome background using Gene Ontology (GO) Biological Process (BP) and WikiPathways databases (43). GO BP terms and WikiPathways were considered significantly enriched at Benjamini–Hochberg adjusted $P < 0.05$. Overrepresentation analysis results are provided in Supplemental File S2. Network plots were generated using the GO BP overrepresentation data with *cnetplot* function in clusterProfiler. Heatmaps were generated using trimmed mean of *M* values (TMM)-normalized and log2-transformed gene counts with the "pheatmap" package (https://CRAN.R-project.org/package=pheatmap) with scaling by row and complete clustering of rows and columns by Euclidean distance. Principal components analysis (PCA) plot of TMM-normalized and transformed (*vst* function in DESeq2) gene expression data was created using the *plotPCA* function in DESeq2. Differences in TMM-normalized and log2-transformed counts of specific genes between treatments were analyzed using linear mixed-effects models (LMM) with treatment as a fixed effect and animal from which PCATS were obtained as a random effect ["lme4" and "lmerTest" packages (44)]. Post hoc tests were conducted using estimated marginal means (with Benjamini–Hochberg adjustment for multiple comparisons) with the "emmeans" package (45). Model residuals were visually assessed for homoscedasticity and normality. Daily BPA consumption by NES was estimated using published foraging data and measured BPA levels in myctophids (28, 30), as follows: 1,000 feeding events/day × 10 g BPA/fish × 20% of fish with detected BPA levels × 1 ng/g BPA in fish = ~2 μg BPA consumed/day.

RESULTS

The NES PCATS transcriptome assembly contained 1,413,571 contigs (transcripts) with a median contig length of 423 base pairs, of which 85.3% had significant sequence similarity to highly conserved mammalian genes (Benchmarking Universal Single-Copy Orthologs, BUSCOs), suggesting high assembly completeness. Of the assembled transcripts, 84,418 that were expressed at ≥10 transcripts per million (TPM) in three or more samples were used for differential expression analyses comparing treatment groups (CORT vs. control, EPI vs. control, CORT-EPI vs. control, BPA vs. control, BPS vs. control, BPA-EPI vs. control, and BPS-EPI vs. control). Because of high interindividual variability in transcriptome profiles (Fig. 2), differences in gene expression between treatments were analyzed with blocking by individual from which PCATS were obtained. CORT, EPI, CORT-EPI, BPA, and BPS treatments altered the expression of 273, 229, 756, 21, and 14 annotated genes in PCATS relative to control, respectively (Fig. 3 and Supplemental File S1). BPA-EPI and BPS-EPI altered expression of 216 and 267 genes relative to control, respectively (Fig. 3). Four genes that were significantly upregulated by all treatments relative to control encoded the catalytic subunit of cAMP-dependent protein kinase A (PRKACA), cyclin-dependent kinase-binding protein CABLES1, cAMP-degrading enzyme PDE8A, and histone methyltransferase KMT2D.

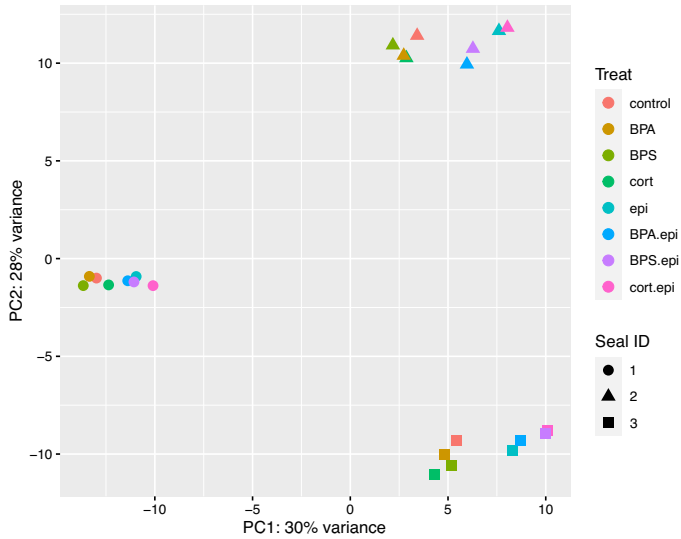

Figure 2. Principal components analysis (PCA) plot of elephant seal precision-cut adipose tissue slices (PCATS) gene expression data. Gene counts were normalized by library size (trimmed mean of *M* values, TMM) and transformed (variance stabilizing transformation) using DESeq2. Different colors denote culture treatments, whereas different symbol shapes denote individual seals from which PCATS were obtained. BPA, bisphenol A; BPS, bisphenol S; CORT, cortisol; EPI, epinephrine.

Blubber Response to Stress Hormones

CORT, EPI, and CORT-EPI altered expression of a total of 996 genes in PCATS relative to control treatment, including multiple isoforms of the same genes. Seventeen DEG were upregulated in response to all three stress hormone treatments, including the four that were also regulated by bisphenols (Fig. 4). These genes were associated with lipolysis (*AQP7*), fatty acid oxidation (*HMGCS2*), lipogenesis (*THRSP*), thermogenesis (*ALPL*), negative regulation of inflammation (*TSC22D3*) and gluconeogenesis (*FAM3D*), regulation of nuclear hormone receptor activity (*PELP1*), proteolysis (*TGM2*), extracellular matrix (ECM) organization (*CRISPLD2*), xenobiotic metabolism (*FMO4*), transmembrane voltage sensing (*TMEM266*), and GPCR downregulation (*ARRDC2*).

CORT treatment alone caused upregulation of 183 and downregulation of 61 genes relative to control, of which 149 were not detected in any other comparison (Fig. 3 and Supplemental File S1). CORT-regulated DEG included 37 that were identified in a previous in vivo study of the effects of ACTH administration on the blubber transcriptome of juvenile NES [e.g., *ACSM1*, *AZGP1*, *CDO1*, *CEBPD*, *DDK1*, *FAM3D*, *FKBP5*, *GPX3*, *HMGCS2*, *KLF9*, *LEP*, *MOGAT3*, *PER1*, and *ZBTB16;* (19, 20)]. The top most significantly overrepresented GO BP terms in the CORT-regulated DEG set ($n = 136$) were response to steroid hormone, cellular response to organic cyclic compound, blood vessel development, positive regulation of cell migration, and positive regulation of cell motility (Fig. 5 and Supplemental File S2). WikiPathways that were overrepresented among the CORT versus control DEG set ($n = 5$) included TGFB/Smad signaling pathway, complement and coagulation cascades, and microglia pathogen phagocytosis pathway (Supplemental File S2). Manual search of DEG functions of relevance to marine mammal physiology identified specific CORT-regulated genes of interest

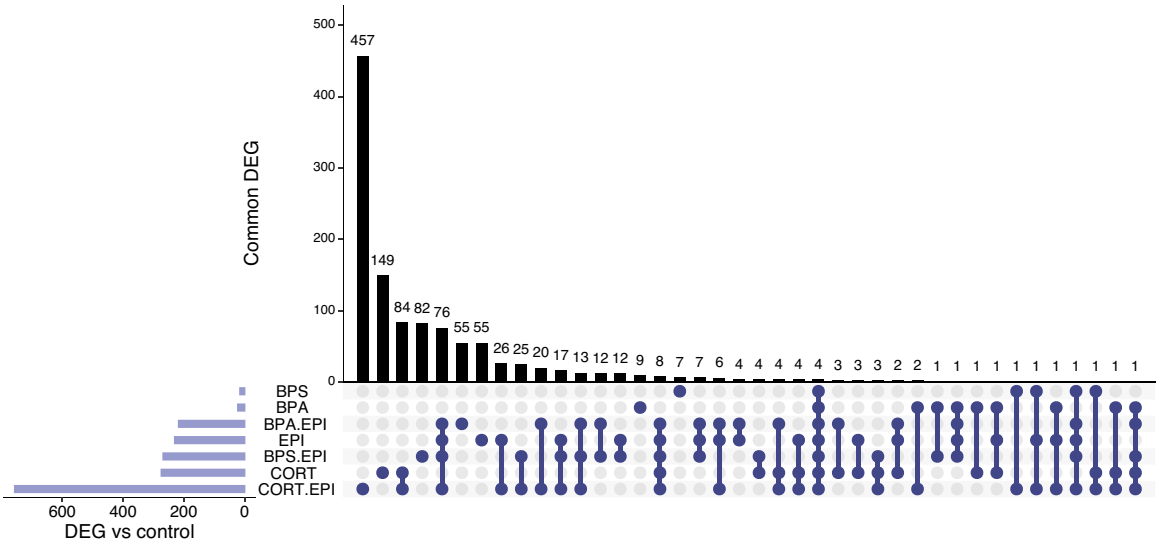

Figure 3. UpSet plot showing overlap in sets of differentially expressed genes (DEGs; log2 fold change > |1|, adj. $P < 0.1$) in precision-cut adipose tissue slices (PCATS) from weaned elephant seal pups ($n = 3$) in response to cortisol (CORT), epinephrine (EPI), CORT-EPI, bisphenol A (BPA), bisphenol S (BPS), BPA-EPI, and BPS-EPI treatments (relative to control). Connections between dots indicate that DEGs were shared between conditions, whereas unconnected dots show unique DEGs for each condition. The bars on the left indicate the number of DEGs identified in each treatment, whereas the columns at the top show number of DEGs that were either unique or shared between treatments.

(Table 1) that were associated with adipokine signaling; adipogenesis; angiogenesis; BMP signaling; circadian clock; GPCR and cAMP-dependent signaling; immune function; lipid catabolism, synthesis, and transport; protein synthesis; redox homeostasis; regulation of apoptosis and autophagy; regulation of estrogen and insulin signaling; response to histamine and serotonin; and thermogenesis.

EPI treatment alone caused upregulation of 146 and downregulation of 55 genes in PCATS relative to control, of which 55 were not detected in any other comparison (Fig. 3 and Supplemental File S1). These included 8 "immediate-early" norepinephrine-responsive genes identified in human adipocytes (*CREM*, *NR4A1*, *NR4A2*, *NR4A3*, *JMY*, *MSC*, *NCOR2*, and *POLR2A*; (46)). The top most significantly overrepresented GO BP terms in the EPI-regulated DEG ($n = 154$) set were response to extracellular stimulus, response to nutrient levels, fatty acid oxidation, lipid oxidation, response to starvation, response to steroid hormone, and intracellular receptor signaling pathway (Fig. 6 and Supplemental File S2). WikiPathways that were overrepresented in the EPI versus control DEG set ($n = 6$) included PPAR signaling pathway, nuclear receptors, adipogenesis, and estrogen receptor pathway (Supplemental File S2). Manual search of DEG functions identified specific EPI-regulated genes of interest (Table 2) that were associated with adipokine signaling; amino acid catabolism; regulation of angiogenesis, apoptosis, and autophagy; electron transport chain; embryonic development; fatty acid oxidation; GPCR and

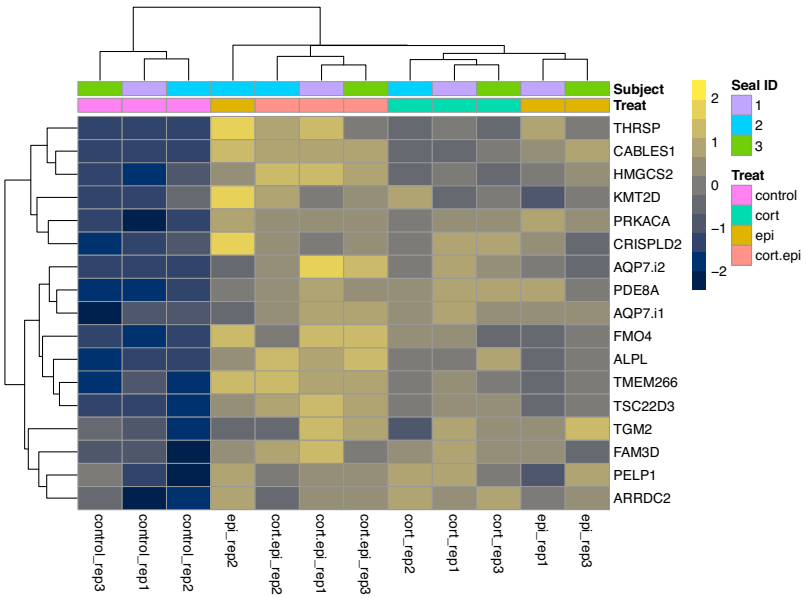

Figure 4. Heatmap showing scaled relative expression of 17 transcripts that were differentially expressed in response to cortisol (CORT), epinephrine (EPI), and CORT-EPI treatments (relative to control) in elephant seal precision-cut adipose tissue slices (PCATS). Rows and columns were clustered by Euclidian distance.

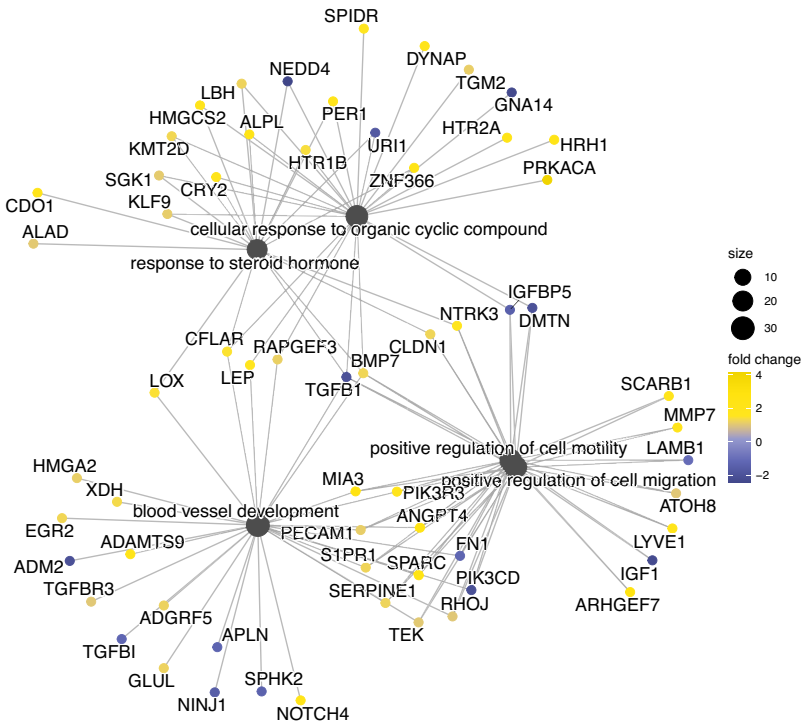

Figure 5. Network plot of Gene Ontology (GO) Biological Process (BP) terms that were overrepresented (*P*.adj < 0.05) among cortisol (CORT)-regulated genes in elephant seal precision-cut adipose tissue slices (PCATS). Genes that were upregulated in response to CORT treatment relative to control are shown in yellow, whereas those that were downregulated are shown in blue. Size refers to the number of genes mapping to each GO BP term.

cAMP-dependent signaling; immune function and inflammation; lipogenesis; lipolysis; mRNA processing; negative regulation of adipogenesis; nuclear receptor signaling; protein synthesis; regulation of cell cycle, glucose metabolism, and transcription; and response to a variety of neuroendocrine signals (Table 2). One downregulated transcript was annotated as *PRKACA* ("*PRKACA.i2*") and was distinct from the *PRKACA* transcript that was upregulated in all treatment conditions ("*PRKACA.i1*"). Sequence alignment demonstrated that *PRKACA.i2* was a reverse complement of *PRKACA.i1*, which may be an artifact of the de novo transcriptome assembly.

The CORT-EPI combination treatment caused upregulation of 420 and downregulation of 222 genes in PCATS, of which 457 were not identified in any other comparison (Fig. 3 and Supplemental File S1). The top most significantly overrepresented GO BP terms in the CORT-EPI versus control DEG set ($n = 274$) were circulatory system process, blood circulation, vascular process in circulatory system, response to steroid hormone, cellular response to organonitrogen compound, and regulation of lipid metabolic process (Fig. 7 and Supplemental File S2). The only WikiPathway that was overrepresented in the CORT-EPI DEG set was PPAR signaling pathway (Supplemental File S2). Specific genes of interest that were differentially expressed solely in response to CORT-EPI (Table 3) included those associated with adipogenesis; adipokine signaling; adrenergic receptor signaling; antioxidant function; apoptosis; caveolae formation; cell cycle; corticosteroid biosynthesis; electron transport chain; fatty acid metabolism and transport; glycogen synthesis; inflammation and immune response; lipid droplet organization; lipid synthesis and storage; lipolysis; nitric oxide pathway; pentose phosphate pathway; protein synthesis; protein ubiquitination and degradation; regulation of nuclear hormone receptor activity, PI3K-Akt-mTOR pathway, and growth hormone signaling; response to a variety of neuroendocrine signals; unfolded protein response; and Wnt signaling pathway.

Blubber Response to Bisphenols

BPA and BPS had a less pronounced effect on PCATS gene expression than stress hormones. Only 21 and 14 transcripts were differentially expressed in response to BPA and BPS treatments alone relative to control, respectively (Fig. 3 and Supplemental File S1). To increase our chance of discovery of bisphenol-regulated genes, we also examined DEG that had log2 fold changes < |1|, as fold changes < 2 may be biologically significant (47). BPA and BPS each affected distinct groups of genes (i.e., there were no DEG shared between BPA vs. control and BPS vs. control gene sets, other than 4 genes that were identified in all treatments). BPA-responsive genes (Table 4) included eight that were also differentially expressed in response to treatment with CORT, EPI, and/or CORT-EPI. Genes that were uniquely upregulated by BPA treatment included the cytokine *CXCL14*, mTOR pathway inhibitor *DDIT4L*, sodium ion channel regulator *SCN4B*, cell migration regulator *FAM110C*, and calcium ion pump *ATP2C2* (Fig. 8). Genes that were uniquely downregulated by BPA treatment included the ceramide biosynthesis enzyme *SGMS2*, calcium channel regulator *STIMATE*, amino acid symporter *SLC38A5*, and *FAM25C* (function unknown). BPS-responsive genes (Table 4) included four that were differentially expressed in response to CORT, EPI, and/or CORT-EPI treatments. Genes that were uniquely differentially expressed in response to BPS treatment (Fig. 8) included the transcriptional regulator *THAP3*, mediator of TNF- and reactive oxygen species (ROS)-induced necrosis *PGAM5*, BMP

Table 1. *Genes of interest differentially expressed in CORT-treated precision-cut adipose tissue slices from weaned northern elephant seal pups*

Transcript ID	Gene Symbol	log2 Fold Change	Putative Function
TRINITY_DN9747_c0_g1	*APLN*	−1.27	Adipokine signaling
TRINITY_DN20796_c0_g1	*ZBTB16*	3.90	Adipogenesis
TRINITY_DN8115_c0_g3	*SFRP5*	2.80	Adipogenesis
TRINITY_DN909_c0_g1	*CDO1*	2.06	Adipogenesis
TRINITY_DN3720_c0_g1	*DKK1*	1.25	Adipogenesis
TRINITY_DN5705_c0_g1	*KLF9*	1.10	Adipogenesis
TRINITY_DN5425_c0_g2	*TGFBI*	−1.22	Adipogenesis
TRINITY_DN6067_c1_g2	*ANGPT4*	2.38	Angiogenesis
TRINITY_DN11004_c0_g1	*TEK*	1.03	Angiogenesis
TRINITY_DN3899_c3_g1	*BMP7*	1.25	BMP signaling pathway
TRINITY_DN8468_c0_g1	*PER1*	2.11	Circadian clock
TRINITY_DN3543_c0_g3	*CRY2*	1.89	Circadian clock
TRINITY_DN5306_c0_g1	*PDE1A*	1.66	GPCR and cAMP-dependent signaling
TRINITY_DN3307_c0_g2	*CD209L2*	2.86	Immune function and inflammation
TRINITY_DN15672_c0_g1	*BTNL9*	2.49	Immune function and inflammation
TRINITY_DN34771_c0_g1	*IL10RA*	2.41	Immune function and inflammation
TRINITY_DN61440_c0_g1	*C1QA*	1.53	Immune function and inflammation
TRINITY_DN11934_c0_g1	*NFKBIA*	1.13	Immune function and inflammation
TRINITY_DN505_c1_g1	*ACSM1*	3.28	Lipid catabolism
TRINITY_DN22758_c0_g1	*ACOX2*	2.71	Lipid catabolism
TRINITY_DN931_c0_g3	*AQP7*	1.78	Lipid catabolism
TRINITY_DN22991_c3_g1	*ACSL1*	1.30	Lipid catabolism
TRINITY_DN855_c0_g1	*AZGP1*	1.05	Lipid catabolism
TRINITY_DN22059_c0_g1	*MOGAT3*	2.26	Lipid synthesis
TRINITY_DN2269_c0_g1	*THRSP*	1.16	Lipid synthesis
TRINITY_DN6384_c0_g1	*SCARB1*	1.88	Lipid transport
TRINITY_DN24505_c1_g1	*APOL6*	1.03	Lipid transport
TRINITY_DN14819_c2_g1	*IGFBP5*	−1.43	Protein synthesis
TRINITY_DN8073_c0_g1	*IGF1*	−2.25	Protein synthesis
TRINITY_DN14282_c0_g2	*GPX3*	3.19	Redox homeostasis
TRINITY_DN1019_c4_g1	*XDH*	1.32	Redox homeostasis
TRINITY_DN3575_c0_g2	*DEPP1*	2.38	Regulation of apoptosis and autophagy
TRINITY_DN27679_c0_g1	*EDAR*	2.16	Regulation of apoptosis and autophagy
TRINITY_DN4547_c5_g1	*CFLAR*	1.45	Regulation of apoptosis and autophagy
TRINITY_DN439_c4_g1	*BCL2L12*	−1.94	Regulation of apoptosis and autophagy
TRINITY_DN72109_c3_g1	*ZNF366*	2.37	Regulation of estrogen signaling
TRINITY_DN7629_c0_g1	*PIK3R3*	1.83	Regulation of insulin receptor pathway
TRINITY_DN6225_c0_g1	*PTPRE*	1.19	Regulation of insulin receptor pathway
TRINITY_DN73275_c4_g1	*HRH1*	2.22	Response to histamine
TRINITY_DN11085_c0_g1	*HTR2A*	2.34	Response to serotonin
TRINITY_DN2004_c1_g2	*HTR1B*	1.39	Response to serotonin
TRINITY_DN3778_c0_g1	*TGFBR3*	1.01	TGF-β signaling pathway
TRINITY_DN42444_c0_g2	*ALPL*	2.32	Thermogenesis

Putative functions of proteins encoded by differentially expressed genes were obtained from UniProt. The complete differentially expressed genes list is in Supplemental File S1. $n = 3$ pups; relative to control. CORT, cortisol; GPCR, protein-coupled receptor.

coreceptor *RGMB*, GTPase signaling regulator *PLEKHG1*, selenium-responsive gene *SELENOV*, and *CCDC194* (function unknown), which were all downregulated (Fig. 8). In addition, steroid hormone biosynthesis enzyme *HSD17B7* was downregulated by 1.8-fold in response to BPS.

To identify genes that were only regulated by the combination of EPI and bisphenols, we compared PCATS treated with BPA-EPI and BPS-EPI to control. We identified 55 and 82 DEGs in BPA-EPI-and BPS-EPI-exposed PCATS relative to controls, respectively, which were not identified in any other hormone treatment (Fig. 3 and Supplemental File S1). Of these, 10 upregulated DEGs were shared between BPA-EPI- and BPS-EPI-treated blubber slices, which were associated with intracellular protein trafficking (*ARF5*), protein depalmitoylation (*ADBH10*), cell adhesion (*CEACAM1*), neural development (*GFRA1*, *SSPO*), GPCR signaling (*GPR78*), pentose phosphate pathway (*RBKS*), negative regulation of the MAP kinase pathway (*SPRED2*), regulation of transcription (*TEAD1*), and ECM (*COL13A1*). Genes of interest that were differentially regulated only in response to BPA-EPI relative to control (Table 5) included those involved in the BMP signaling pathway, cell proliferation and apoptosis, glucose uptake and glycolysis, immune response and inflammation, inhibition of IGF signaling, oxidation of fatty acids and steroids, regulation of steroid hormone receptors (including GR), and response to DNA damage. Genes of interest that were differentially regulated only in response to BPS-EPI relative to control (Table 5) included those associated with antioxidant function, autophagy, fatty acid oxidation, gluconeogenesis, glycogen synthesis, chaperoning of heat shock proteins, immune response and inflammation, regulation of the cell cycle, response to DNA damage, unfolded protein response, and Wnt signaling pathway. Both BPA-EPI and BPS-EPI caused the downregulation of genes associated with primary cilia, one of which was the most highly downregulated gene in BPS-EPI-treated PCATS (Table 5).

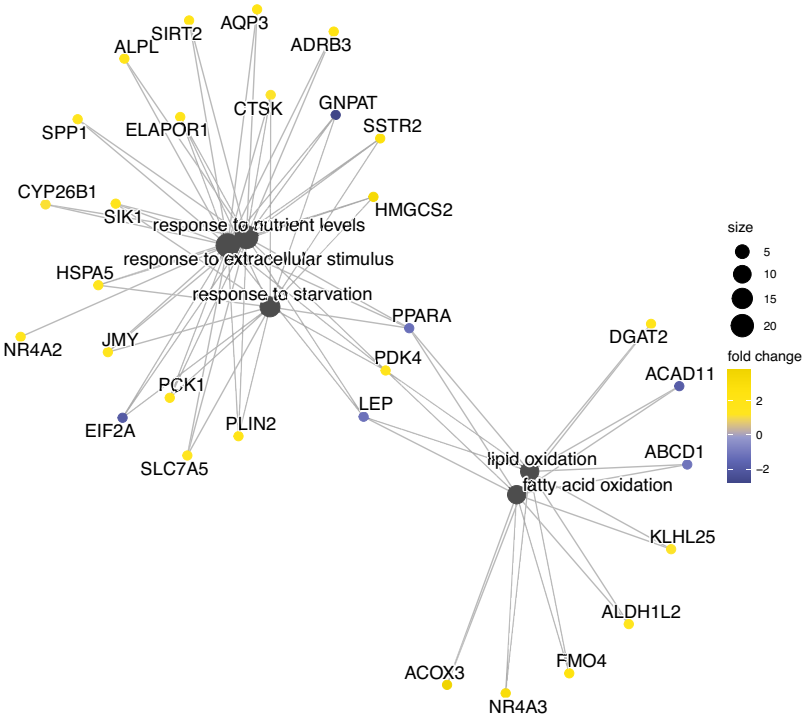

Figure 6. Network plot of Gene Ontology (GO) Biological Process (BP) terms that were overrepresented (*P*.adj $<$ 0.05) among epinephrine (EPI)-regulated genes in elephant seal precision-cut adipose tissue slices (PCATS; $n = 3$). Genes that were upregulated in response to EPI treatment relative to control are shown in yellow, whereas those that were downregulated are shown in blue. Size refers to the number of genes mapping to each GO BP term.

Potential Interactions between Stress Hormones and Bisphenols

To identify potential interactive effects of CORT and EPI on gene expression in PCATS, we first compared mean log2 fold changes of 17 DEGs that were identified in the CORT versus control, EPI versus control, and CORT-EPI versus control comparisons. We broadly defined additive effects as δ = CORT-EPI − (CORT + EPI) = 0, potential synergistic effects as $\delta > 0$, and antagonistic effects as $\delta < 0$. Three genes (*ALPL*, *HMGCS2*, and *TSC22D3*) suggested potential additive effects of CORT and EPI on their expression (Supplemental Fig. S1), whereas the remaining 15 genes suggested antagonistic interactions between the two hormones (e.g., 4 genes shown in Fig. 9). To detect more nuanced interaction effects, we also reran DESeq2 with an interaction term (CORT × EPI). We identified seven annotated DEG with log2 fold change > 0, suggesting synergistic effects, and 10 DEGs with log2 fold change < 0, suggesting antagonistic effects (Supplemental File S3). The predicted functions of genes that were synergistically regulated by CORT and EPI included negative regulation of Wnt and GPCR signaling, immune function, and glyceroneogenesis. Genes antagonistically regulated by CORT and EPI were associated with angiogenesis, adipogenesis, epigenetic regulation of gene expression, and NF-κB signaling, among others (Table 6).

To identify potential interactive effects of bisphenols and EPI on gene expression in PCATS, we first compared mean log2 fold changes of DEGs that were identified in the BPA/S versus control, EPI versus control, and BPA/S-EPI versus control comparisons. The bisphenols showed potential antagonistic effects with EPI (all $\delta < -1.3$) on expression of four DEGs common to all of the comparisons: *CABLES1*, *PRKACA*, *PDE8A*, and *KMT2D* (Fig. 9). In addition, BPA and EPI showed potential antagonism on *SPP1* expression ($\delta = -1.3$), whereas BPS and EPI showed a potentially antagonistic effect ($\delta = -1.7$) on expression of a downregulated gene annotated as *RHO* (rhodopsin). DESeq2 identified one additional gene that was synergistically regulated by BPA and EPI (*HNRNPM*) and one that was synergistically regulated by BPS and EPI (*RBM6*); both are associated with mRNA binding and processing. The chemokine *CXCL14* was identified as antagonistically regulated by BPA and EPI, whereas three genes antagonistically regulated by BPS and EPI were involved in DNA damage response (*ERCC6L2*), NAD(P)H damage repair (*NAXE*), and ubiquinone biosynthesis (*COQ4*; Table 6).

DISCUSSION

Our understanding of the effects of multiple stressors on the physiology of marine mammals has been hindered by the practical and ethical challenges of conducting functional studies in free-ranging, large, fully aquatic, and federally protected species. Moreover, previous marine mammal stress studies have largely ignored the role of the SAM system in molecular responses to stress and its interactions with the HPA axis and anthropogenic contaminants, in part due to the rapid release and short half-life of catecholamines. A biologically relevant ex vivo system can address these challenges by enabling controlled and combinatorial stressor experiments that are impractical to conduct in vivo. We previously developed a marine mammal blubber slice culture system that preserves tissue architecture and biological function ex vivo (31). In this study, we used this system to examine the individual and combinatorial effects of CORT, EPI, and the bisphenol additives/monomers BPA and BPS on global gene expression profiles in blubber from weaned NES pups. We found that PCATS retained molecular characteristics of the source individuals and demonstrated a transcriptional response to CORT that mirrored that which we previously reported in vivo. We identified core groups of blubber genes that were differentially regulated

Table 2. *Genes of interest differentially expressed in EPI-treated precision-cut adipose tissue slices from weaned northern elephant seal pups*

Transcript ID	Gene Symbol	log2 Fold Change	Putative Function
TRINITY_DN4852_c0_g2	*ANGPTL4*	1.58	Adipokine signaling
TRINITY_DN851_c2_g1	*LEP*	−1.22	Adipokine signaling
TRINITY_DN573_c0_g2	*TDH*	2.46	Amino acid catabolism
TRINITY_DN12162_c2_g1	*WARS1*	1.40	Angiogenesis
TRINITY_DN458874_c0_g1	*SOX18*	−1.02	Angiogenesis
TRINITY_DN5153_c1_g1	*HEG1*	−2.95	Angiogenesis
TRINITY_DN67025_c1_g2	*ELAPOR1*	1.66	Apoptosis and autophagy
TRINITY_DN30946_c0_g1	*XKR6*	−1.06	Apoptosis and autophagy
TRINITY_DN11030_c0_g1	*NDUFAF6*	−1.77	Electron transport chain
TRINITY_DN9508_c1_g1	*NOG*	2.28	Embryonic development
TRINITY_DN56650_c1_g2	*PAX1*	2.22	Embryonic development
TRINITY_DN664_c0_g2	*HOXB9*	1.03	Embryonic development
TRINITY_DN745845_c1_g1	*NODAL*	1.01	Embryonic development
TRINITY_DN28487_c0_g1	*HMGCS2*	3.28	Fatty acid oxidation
TRINITY_DN713_c0_g3	*ACOX3*	1.56	Fatty acid oxidation
TRINITY_DN9251_c0_g1	*ALDH1L2*	1.33	Fatty acid oxidation
TRINITY_DN1605_c0_g1	*ABCD1*	−1.15	Fatty acid oxidation
TRINITY_DN50635_c0_g1	*ACAD11*	−1.83	Fatty acid oxidation
TRINITY_DN7566_c0_g2	*PRKACA.i1*	4.88	GPCR and cAMP-dependent signaling
TRINITY_DN648_c0_g1	*PRKACA.i2*	−3.55	GPCR and cAMP-dependent signaling
TRINITY_DN4279_c1_g1	*ADRB3*	2.24	GPCR and cAMP-dependent signaling
TRINITY_DN26499_c0_g1	*PDE10A*	2.15	GPCR and cAMP-dependent signaling
TRINITY_DN5346_c1_g1	*ADCY5*	2.13	GPCR and cAMP-dependent signaling
TRINITY_DN10085_c0_g1	*CAMK1G*	1.26	GPCR and cAMP-dependent signaling
TRINITY_DN2983_c0_g4	*ARRDC4*	−1.58	GPCR and cAMP-dependent signaling
TRINITY_DN518_c0_g2	*CXCL8*	2.40	Immune function and inflammation
TRINITY_DN9803_c0_g1	*CXCR4*	1.12	Immune function and inflammation
TRINITY_DN9683_c0_g2	*C1QBP*	−1.07	Immune function and inflammation
TRINITY_DN4215_c0_g1	*IL17RE*	−2.23	Immune function and inflammation
TRINITY_DN2269_c0_g1	*THRSP*	2.50	Lipogenesis
TRINITY_DN18919_c0_g1	*PPARA*	−1.27	Lipogenesis
TRINITY_DN1061_c2_g1	*PLIN2*	1.99	Lipolysis
TRINITY_DN4487_c0_g1	*AQP3*	1.97	Lipolysis
TRINITY_DN931_c0_g3	*AQP7*	1.52	Lipolysis
TRINITY_DN5876_c0_g3	*G0S2*	1.24	Lipolysis
TRINITY_DN3038_c1_g1	*AZGP1*	1.00	Lipolysis
TRINITY_DN35156_c0_g1	*RBM5*	−1.00	mRNA processing
TRINITY_DN20777_c0_g1	*TRIB3*	1.21	Negative regulation of adipogenesis
TRINITY_DN1958_c1_g1	*ASXL1*	−1.11	Negative regulation of adipogenesis
TRINITY_DN5027_c2_g3	*NR4A3*	2.97	Nuclear receptor signaling
TRINITY_DN152_c0_g1	*NR1H3*	1.41	Nuclear receptor signaling
TRINITY_DN3184_c2_g1	*NR4A2*	1.31	Nuclear receptor signaling
TRINITY_DN1845_c5_g1	*NR4A1*	1.27	Nuclear receptor signaling
TRINITY_DN126365_c0_g2	*EIF2A*	−1.95	Protein synthesis
TRINITY_DN30944_c0_g1	*CDC23*	−1.93	Regulation of cell cycle
TRINITY_DN3950_c0_g1	*CABLES2*	−3.41	Regulation of cell cycle
TRINITY_DN5084_c0_g2	*PCK1*	1.48	Regulation of glucose metabolism
TRINITY_DN9514_c1_g3	*PDK4*	1.58	Regulation of glucose metabolism
TRINITY_DN1905_c0_g2	*SIK1*	1.55	Regulation of glucose metabolism
TRINITY_DN3549_c0_g3	*GFPT2*	1.76	Regulation of glucose metabolism
TRINITY_DN18478_c0_g1	*SIRT2*	1.78	Regulation of glucose metabolism
TRINITY_DN19330_c1_g1	*IGFBP3*	1.37	Regulation of glucose metabolism
TRINITY_DN7162_c0_g2	*NCOR2*	2.32	Regulation of transcription
TRINITY_DN923_c0_g1	*JMY*	1.24	Regulation of transcription
TRINITY_DN7142_c1_g1	*RCOR1*	−3.18	Regulation of transcription
TRINITY_DN12802_c0_g1	*CHRM4*	1.81	Response to acetylcholine
TRINITY_DN206393_c0_g1	*EDNRB*	1.13	Response to endothelin
TRINITY_DN7591_c0_g1	*ESR1*	1.39	Response to estrogen
TRINITY_DN5870_c0_g2	*HCAR2*	1.20	Response to hydroxycarboxylic acid
TRINITY_DN10150_c0_g1	*HTR1B*	−1.62	Response to serotonin
TRINITY_DN9772_c0_g1	*SSTR2*	2.63	Response to somatostatin
TRINITY_DN25855_c0_g1	*TACR1*	3.09	Response to substance P
TRINITY_DN3439_c0_g1	*DHH*	−1.81	Steroid biosynthesis
TRINITY_DN34431_c0_g1	*GLCCI1*	−1.67	Transcriptional response to GCs
TRINITY_DN20119_c0_g2	*DGAT2*	2.66	Triglyceride synthesis
TRINITY_DN5808_c0_g1	*GPAT3*	1.07	Triglyceride synthesis

Putative functions of proteins encoded by differentially expressed genes were obtained from UniProt. The complete differentially expressed genes list is in Supplemental File S1. $n = 3$ pups; relative to control. EPI, epinephrine; GC, glucocorticoid; GPCR, protein-coupled receptor.

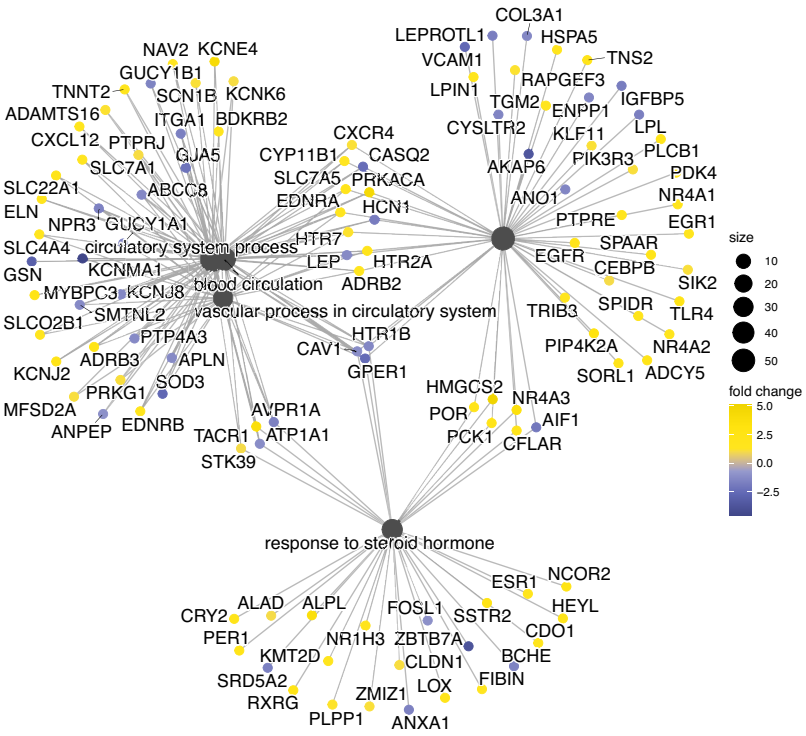

Figure 7. Network plot of Gene Ontology (GO) Biological Process (BP) terms that were overrepresented (*P*.adj < 0.05) among cortisol-epinephrine (CORT-EPI)-regulated genes in elephant seal precision-cut adipose tissue slices (PCATS; $n = 3$). Genes that were upregulated in response to CORT-EPI treatment relative to control are shown in yellow, whereas those that were downregulated are shown in blue. Size refers to the number of genes mapping to each GO BP term.

by all stressors, stressor-specific genes that responded to particular hormones or contaminants, and potential evidence of interactions between hormones and contaminants on gene expression. Differentially expressed genes were associated with metabolic and cellular homeostasis, regulation of hormone sensitivity and signaling, immune response, and other functions, with implications for consequences of stress exposure on physiology of marine mammals. We suggest that future work using the PCATS system broaden our understanding of stress effects on blubber physiology by including samples from animals of varying life history stages and sexes. This would provide information on how ontogeny and life history shape stress responses and enable more direct comparisons with in vivo studies in NES.

Common Response of Blubber to Stressors

Four genes (*PRKACA*, *PDE8A*, *CABLES1*, and *KMT2D*) were upregulated in PCATS in response to all treatments and their combinations tested, suggesting that they may be potential core markers of stress responses. The combination treatments showed the potential for antagonistic effects of CORT and EPI and of bisphenols and EPI on their expression, suggesting that the simultaneous presence of GCs and/or contaminants with catecholamines may limit blubber responses to the latter. *PRKACA* encodes the catalytic subunit of PKA, which is activated in response to ligands that bind to GPCRs (e.g., catecholamines, ACTH) and functions to stimulate lipolysis, thermogenesis, glucose uptake, and glycolysis (48). We previously found that PRKACA protein abundance increased in response to ACTH stimulation in NES blubber in vivo (49), and Fang et al. (50) recently reported that mouse adipocytes also upregulate *PRKACA* in response to BPA. Therefore, *PRKACA* upregulation suggests that GPCR activation is a common feature of blubber responses to hormones and contaminants. This response is regulated by intracellular negative feedback, as evidenced by the upregulation of *PDE8A*, a phosphodiesterase that inhibits PKA activity by degrading cAMP (51). Upregulation of *CABLES1* and *KMT2D*, which mediate the growth-suppressing effects of GCs and restrict proliferation and differentiation of B cells, respectively (52, 53), may lead to impaired cell turnover and immune function in blubber in response to stress. These results suggest that CORT, EPI, bisphenols, and their combinations may impact cellular, immune, and metabolic homeostasis in marine mammal blubber, which may impact the ability of capital breeding marine mammals to sustain prolonged fasting, renew tissues, and mount appropriate responses to immune challenges.

Thirteen genes responded to all hormone treatments (CORT, EPI, and CORT-EPI), but not bisphenols, and included several key regulators of lipid and immune homeostasis, such as *ALPL*, *THRSP*, *HMGCS2*, *FAM3D*, and *TSC22D3*. *HMGCS2* and *FAM3D* were also upregulated in blubber in vivo in response to ACTH (19, 20). *ALPL* and *TSC22D3* are induced by GC and adrenergic receptors and mediate their effects on adipogenesis, lipolysis, thermogenesis, adipokine production, and immunity (54, 55), whereas *THRSP* and *HMGCS2* stimulate fatty acid oxidation and mitochondrial respiration in adipose tissue (55, 56). Upregulation of these genes in PCATS highlights the wide-ranging effects of stress hormones on metabolism and suggests that they are potential molecular indicators of elevated CORT and EPI in marine mammal blubber. CORT and EPI showed potential for additive effects on expression of *ALPL*, *HMGCS2*, and *TSC22D3*, which suggests that lipid catabolism is maximally activated in the presence of both stress hormones, albeit via noninteracting pathways. Two other genes upregulated by CORT, EPI, and CORT-EPI treatments, *PELP1* and *ARRDC2*, inhibit the transcriptional

Table 3. *Genes of interest differentially expressed in CORT-EPI-treated precision-cut adipose tissue slices from weaned northern elephant seal pups*

Transcript ID	Gene Symbol	log2 Fold Change	Putative Function
TRINITY_DN5512_c0_g1	*PPARGC1A*	2.17	Adipogenesis
TRINITY_DN7433_c0_g3	*ZNF385A*	1.02	Adipogenesis
TRINITY_DN4559_c0_g3	*CEBPB*	1.00	Adipogenesis
TRINITY_DN3444_c5_g1	*ZBTB7A*	−3.74	Adipogenesis
TRINITY_DN3567_c0_g1	*C1QTNF3*	−1.79	Adipokine signaling
TRINITY_DN1018_c1_g2	*GRK3*	2.46	Adrenergic receptor signaling
TRINITY_DN4217_c0_g2	*LRP8*	1.83	Adrenergic receptor signaling
TRINITY_DN5876_c1_g1	*FHL5*	1.70	Adrenergic receptor signaling
TRINITY_DN20089_c0_g1	*ADRB2*	1.28	Adrenergic receptor signaling
TRINITY_DN6223_c0_g1	*GGA2*	1.03	Adrenergic receptor signaling
TRINITY_DN601_c0_g1	*PRDX5*	−1.42	Antioxidant function
TRINITY_DN24555_c0_g2	*SOD3*	−2.68	Antioxidant function
TRINITY_DN534_c0_g1	*GADD45G*	1.63	Apoptosis
TRINITY_DN18032_c0_g1	*FOXO3B*	1.27	Apoptosis
TRINITY_DN5082_c0_g3	*HIPK2*	1.17	Apoptosis
TRINITY_DN6179_c0_g1	*BMF*	−1.78	Apoptosis
TRINITY_DN20205_c0_g2	*CAV1*	−1.17	Caveolae formation
TRINITY_DN3551_c0_g2	*MKI67*	1.33	Cell cycle
TRINITY_DN4653_c0_g1	*CDCA7L*	1.09	Cell cycle
TRINITY_DN249120_c0_g1	*POR*	2.08	Corticosteroid biosynthesis
TRINITY_DN771_c0_g1	*CYP11B1*	1.24	Corticosteroid biosynthesis
TRINITY_DN4749_c0_g2	*MT-ND5*	−1.71	Electron transport chain
TRINITY_DN9360_c0_g2	*NDUFA8*	−1.21	Electron transport chain
TRINITY_DN56_c2_g1	*FABP4*	1.19	Fatty acid metabolism and transport
TRINITY_DN19943_c0_g2	*SLC25A20*	1.18	Fatty acid metabolism and transport
TRINITY_DN19658_c0_g1	*SIK2*	1.10	Fatty acid metabolism and transport
TRINITY_DN9849_c0_g1	*ACACA*	1.09	Fatty acid metabolism and transport
TRINITY_DN6427_c0_g1	*ACACB*	−1.60	Fatty acid metabolism and transport
TRINITY_DN3644_c0_g2	*PPP1R3B*	1.18	Glycogen synthesis
TRINITY_DN6847_c0_g1	*PPP1R3C*	−1.05	Glycogen synthesis
TRINITY_DN759138_c0_g1	*TLR4*	2.42	Immune function and inflammation
TRINITY_DN10909_c0_g1	*IL1F10*	2.28	Immune function and inflammation
TRINITY_DN8606_c0_g3	*CXCL12*	1.66	Immune function and inflammation
TRINITY_DN494_c0_g1	*TNFRSF1B*	1.41	Immune function and inflammation
TRINITY_DN448_c0_g4	*CD46*	1.27	Immune function and inflammation
TRINITY_DN27546_c0_g2	*CARD8*	−1.21	Immune function and inflammation
TRINITY_DN64870_c0_g1	*ANXA1*	−1.62	Immune function and inflammation
TRINITY_DN24480_c0_g3	*CIDEB*	1.38	Lipid droplet organization
TRINITY_DN3606_c0_g2	*CIDEC*	4.31	Lipid droplet organization
TRINITY_DN11508_c0_g1	*FITM2*	1.18	Lipid droplet organization
TRINITY_DN20029_c0_g1	*PLIN1*	1.15	Lipid droplet organization
TRINITY_DN2623_c1_g1	*FASN*	−1.13	Lipid synthesis and storage
TRINITY_DN4824_c0_g1	*LPL*	−1.69	Lipid synthesis and storage
TRINITY_DN1471_c0_g2	*LPIN1*	1.62	Lipolysis
TRINITY_DN6120_c0_g1	*PNPLA2*	1.24	Lipolysis
TRINITY_DN10987_c0_g2	*LIPG*	1.07	Lipolysis
TRINITY_DN3336_c0_g1	*GUCY1A1*	−1.47	Nitric oxide pathway
TRINITY_DN11915_c0_g1	*GUCY1B1*	−1.53	Nitric oxide pathway
TRINITY_DN22648_c0_g2	*RPIA*	1.09	Pentose phosphate pathway
TRINITY_DN15345_c0_g1	*TKT*	−1.04	Pentose phosphate pathway
TRINITY_DN380_c2_g2	*EIF1B*	1.49	Protein synthesis
TRINITY_DN468_c0_g3	*RPS11*	1.06	Protein synthesis
TRINITY_DN6235_c0_g2	*ZER1*	3.14	Protein ubiquitination and degradation
TRINITY_DN747553_c0_g1	*UBE3C*	2.78	Protein ubiquitination and degradation
TRINITY_DN5859_c1_g1	*NCOA7*	1.05	Regulation of nuclear hormone receptor activity
TRINITY_DN3482_c0_g3	*ZMIZ1*	1.11	Regulation of nuclear hormone receptor activity
TRINITY_DN7105_c0_g1	*TNS2*	2.10	Regulation of PI3K-Akt-mTOR pathway
TRINITY_DN2496_c0_g2	*PHLDA3*	−1.21	Regulation of PI3K-Akt-mTOR pathway
TRINITY_DN15264_c0_g1	*PIK3IP1*	−2.05	Regulation of PI3K-Akt-mTOR pathway
TRINITY_DN315_c9_g1	*LEPROTL1*	−1.72	Regulation of growth hormone signaling
TRINITY_DN10278_c1_g1	*NPR3*	−1.57	Response to atrial natriuretic peptide
TRINITY_DN6866_c0_g2	*EDNRA*	−1.35	Response to endothelin
TRINITY_DN46685_c0_g1	*GPER1*	−2.50	Response to estrogen
TRINITY_DN8946_c0_g3	*MT1G*	1.07	Response to glucocorticoids
TRINITY_DN18694_c1_g1	*PTH1R*	−1.52	Response to parathyroid hormone
TRINITY_DN10047_c0_g1	*STRA6L*	1.69	Response to RBP4
TRINITY_DN9265_c1_g2	*AVPR1A*	−1.66	Response to vasopressin

Continued

Table 3.— *Continued*

Transcript ID	Gene Symbol	log2 Fold Change	Putative Function
TRINITY_DN32691_c0_g1	*SRD5A2*	−1.67	Testosterone metabolism
TRINITY_DN54593_c0_g2	*CREB3L2*	2.38	Unfolded protein response
TRINITY_DN3324_c4_g1	*WNT11*	1.95	Wnt signaling pathway
TRINITY_DN4873_c0_g2	*TLE6*	2.53	Wnt signaling pathway

Differentially expressed genes shown here were identified only in the CORT-EPI vs. control comparison. Putative functions of proteins encoded by differentially expressed genes were obtained from UniProt. The complete differentially expressed genes list is in Supplemental File S1. $n = 3$ pups; relative to control. CORT-EPI, cortisol-epinephrine.

activity of GR and promote degradation of beta-adrenergic receptors in mice, respectively (57, 58), suggesting additional mechanisms of intracellular negative feedback in response to stress hormones. However, CORT and EPI showed potential antagonistic effects on their expression, with the implication that simultaneous exposure to both hormones may alter the ability of tissues to appropriately regulate stress responses. Therefore, activation of both SAM and HPA axes may lead to rapid depletion of energy stores and impact the ability of marine mammals to sustain energy-demanding life-history stages such as reproduction and migration.

Blubber Response to Cortisol Treatment

The transcriptome response of PCATS to treatment with CORT alone overlapped with that observed in blubber tissue in vivo in response to cortisol elevation by ACTH (19, 20), confirming that PCATS retain biological function in culture and that the ex vivo system can be used to conduct biologically relevant manipulations. The CORT-induced response included 37 of the same genes that were upregulated in response to ACTH in our previous studies, as well as other genes that shared functions with those identified in vivo (e.g., adipogenesis, lipid metabolism, and immune response) and known GR targets. Three genes, *ACSM1*, *CDO1*, and *PER1*, which encode an enzyme that catalyzes fatty acid activation, a taurine biosynthesis enzyme involved in adipogenesis and fatty acid oxidation (59), and a component of the circadian clock, respectively, were upregulated in this study and both of our previous in vivo ACTH administration studies (19, 20), suggesting that they may represent a core response of elephant seal blubber to cortisol elevation. Upregulation of components of the circadian clock network, such as *PER1*, in response to GCs highlights the complexity of blubber tissue

Table 4. *Genes differentially expressed in BPA- and BPS-treated precision-cut adipose tissue slices from weaned northern elephant seal pups*

Transcript ID	Gene Symbol	log2 Fold Change	Putative Function
BPA vs. control			
TRINITY_DN5132_c1_g1	*SGMS2**	−2.86	Ceramide biosynthesis
TRINITY_DN16567_c0_g1	*MLH3*	1.48	DNA repair
TRINITY_DN61846_c0_g2	*CHST15*	1.38	Hexose biosynthesis
TRINITY_DN378_c2_g1	*CXCL14**	5.79	Immune response and inflammation
TRINITY_DN9683_c0_g2	*C1QBP*	−1.23	Immune response and inflammation
TRINITY_DN35062_c0_g2	*SCN4B**	2.99	Ion transport
TRINITY_DN5014_c1_g3	*ATP2C2**	1.01	Ion transport
TRINITY_DN2027_c0_g1	*SLC38A5**	−1.07	Ion transport
TRINITY_DN528_c10_g1	*STIMATE**	−1.19	Ion transport
TRINITY_DN32862_c0_g2	*DDIT4L**	3.03	Negative regulation of mTOR pathway
TRINITY_DN34868_c0_g1	*PLXNA4*	2.34	Neural development and signaling
TRINITY_DN8625_c1_g1	*DLGAP4*	1.78	Neural development and signaling
TRINITY_DN14756_c0_g1	*BTBD6*	−2.46	Neural development and signaling
TRINITY_DN21402_c0_gz	*FAM110C**	1.89	Regulation of cell migration
TRINITY_DN665_c1_g1	*TBC1D8*	−1.61	Regulation of GTPase signaling
TRINITY_DN5761_c0_g1	*SPP1*	1.41	Response to steroid hormones
TRINITY_DN1308_c0_g2	*FAM25C**	−1.21	Unknown
BPA vs. control			
TRINITY_DN15870_c2_g1	*RGMB**	−1.80	BMP signaling pathway
TRINITY_DN4788_c0_g1	*KMT5C*	−1.65	Epigenetic regulation
TRINITY_DN648_c0_g1	*PRKACA.i2*	−2.83	GPCR signaling pathway
TRINITY_DN26459_c0_g1	*TLE4*	2.89	Negative regulation of Wnt signaling
TRINITY_DN15059_c1_g2	*RHO*	−2.44	Phototransduction
TRINITY_DN8696_c0_g1	*PLEKHG1**	−1.34	Regulation of GTPase signaling
TRINITY_DN10007_c0_g1	*THAP3**	−2.29	Regulation of transcription
TRINITY_DN13685_c0_g1	*SELENOV**	−1.29	Response to selenium
TRINITY_DN42299_c0_g2	*HSD17B7**	−0.82	Steroid hormone biosynthesis
TRINITY_DN1662_c0_g4	*PGAM3**	−1.81	TNF- and ROS-induced necrosis
TRINITY_DN8773_c0_g1	*CCDC194**	−1.77	Unknown

Putative functions of proteins encoded by differentially expressed genes were obtained from UniProt. *Differentially expressed genes that were only identified in the BPA vs. control or BPS vs. control comparisons. The complete differentially expressed gene lists are in Supplemental File S1. $n = 3$ pups; relative to control. BPA, bisphenol A; BPS, bisphenol S; GPCR, protein-coupled receptor.

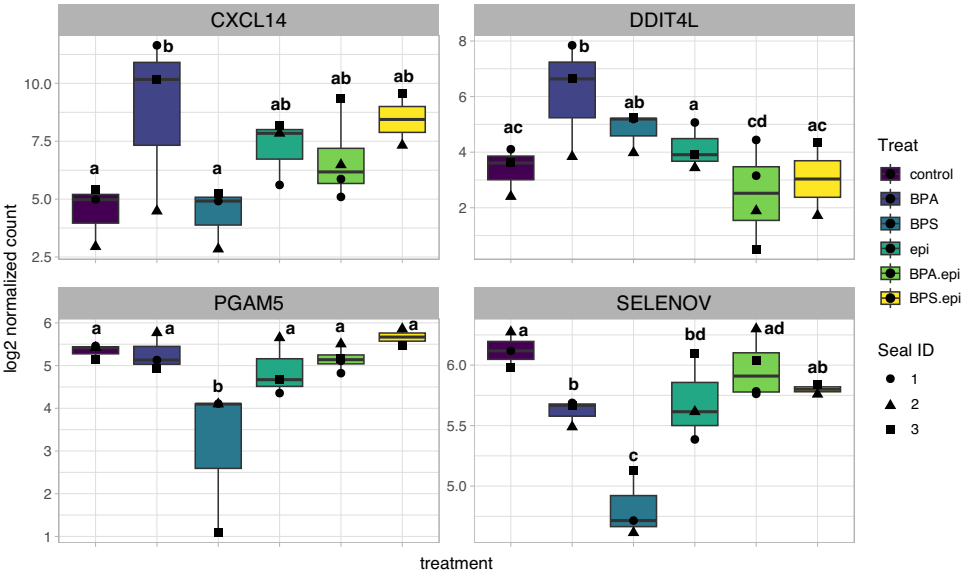

Figure 8. Boxplots showing trimmed mean of *M* values (TMM)-normalized and log2-transformed counts of 4 genes that were differentially expressed in response to bisphenol treatments, but not stress hormones, in elephant seal precision-cut adipose tissue slices (PCATS). Different letters above the boxes denote gene counts that were significantly different between treatments [linear mixed-effects model (LMM) followed by post hoc tests, $P < 0.1$]. Different colors denote PCATS treatments, whereas different symbol shapes denote individual seals from which PCATS were obtained.

and its role in tuning metabolic responses to environmental stimuli, as has been shown in adipose tissue of other mammals (60).

Unlike defined hormone treatments in ex vivo culture, in vivo ACTH administration also affects other hormones: it increases aldosterone and reverse T3 levels and decreases total T3 levels (61). Therefore, identifying genes that were differentially regulated in response to CORT treatment alone ex vivo (but not by ACTH administration in vivo) may enable us to disentangle the effects of cortisol from that of other stress-altered hormones in blubber. For example, CORT treatment, but not ACTH administration, caused downregulation of *IGF1* in blubber, which may serve to promote fat mobilization by inhibiting fat synthesis and storage pathways (62). Further studies will be necessary to identify CORT-specific effects in marine mammal blubber, as differences between DEG sets from different studies may also result from differences in experimental conditions (e.g., magnitude and duration of cortisol elevation and age class of study animals) and transcriptome analysis methods (e.g., different assembler versions, annotation databases, and expression analysis approaches).

Similarly to our in vivo studies and work in other mammals, CORT treatment of PCATS ex vivo altered expression of genes associated with adipogenesis, angiogenesis, ECM remodeling, fatty acid oxidation, and immune function. Other CORT-regulated DEGs included those involved in cAMP-dependent signaling, neurotransmitter catabolism, TGFB and BMP signaling, responses to histamine, serotonin, and IL10, and regulation of estrogen-dependent gene transcription, suggesting that exposure to CORT may influence tissue responsiveness to other neuroendocrine signals. Together, the genes we have identified in both in vivo and ex vivo studies suggest that cortisol elevation in marine mammals likely alters rates of lipid and cellular turnover in blubber, potentially impacting nutrient stores and the ability of animals to respond to additional stressors.

Blubber Response to Epinephrine Treatment

The ex vivo system enabled us to examine the response of blubber tissue to catecholamines, which are frequently overlooked in animal stress studies due to the transient nature of the sympathetic stress response (4). Our previous in vivo ACTH administration studies in elephant seals were conducted under anesthesia, which blunts the sympathetic nervous system response to experimental manipulation, dissociating the HPA and SAM responses (18). Therefore, the physiological consequences of "fight or flight" responses in marine mammals, especially with respect to energy homeostasis, remain unknown. The genomic effects of catecholamines on adipose tissue in other mammals have largely been ignored, with the exception of a recent study that identified a network of immediate-early genes activated in response to 3 h of norepinephrine stimulation in humans (46). In this study, we identified clusters of genes that were differentially expressed in elephant seal blubber in response to EPI treatment alone and the combination of EPI and CORT, including several immediate-early genes induced by norepinephrine in human adipose tissue (46). Other EPI and CORT-EPI-regulated genes included those involved in the response to neuroendocrine signals, including catecholamines and steroid hormones, regulation of lipid and protein turnover, glucose homeostasis, ion and metabolite transport, adipogenesis, cell cycle, apoptosis, immune function, and genetic and epigenetic regulation of gene expression.

Adrenergic signaling.

Treatment of PCATS with EPI caused upregulation of multiple components of the adrenergic signaling pathway, including two β-adrenergic receptor isoforms, several regulators of adrenergic receptor sensitivity, an adenylyl cyclase isoform, cAMP phosphodiesterases, and the cAMP response element modulator *CREM*. Other EPI-upregulated genes included known CREB targets (11), such as the kinases *SIK1* and *SIK2*, nuclear receptors *NR4A1*, *NR4A2*, and *NR4A3*, metabolic regulator *PPARGC1A*, and enzymes *PCK1* and *PDK4*. SIK proteins and NR4A receptors stimulate glucose uptake; inhibit gluconeogenesis, lipogenesis, steroidogenesis, and inflammation; and regulate the activity of other transcription factors such as CREB and PPARG (63, 64). Their upregulation in blubber suggests potential detrimental consequences of

Table 5. *Genes that were differentially expressed only in BPA-EPI- or BPS-EPI-treated precision-cut adipose tissue slices from weaned northern elephant seal pups*

Transcript ID	Gene Symbol	log2 Fold Change	Putative Function
BPA-EPI vs. control			
TRINITY_DN6003_c2_g1	*SMAD9*	−3.99	BMP signaling pathway
TRINITY_DN3381_c2_g1	*BLCAP*	1.93	Cell proliferation and apoptosis
TRINITY_DN11685_c1_g1	*TBC1D1*	4.81	Glucose uptake and glycolysis
TRINITY_DN2347_c1_g1	*HK2*	1.06	Glucose uptake and glycolysis
TRINITY_DN14897_c1_g2	*CD300LF*	3.55	Immune response and inflammation
TRINITY_DN116982_c0_g1	*IKBKB*	2.75	Immune response and inflammation
TRINITY_DN18325_c0_g1	*IGFBP2*	2.77	Inhibition of IGF signaling
TRINITY_DN924_c0_g2	*RDH5*	−1.00	Oxidation of fatty acids and steroids
TRINITY_DN17928_c0_g1	*ACADS*	−2.50	Oxidation of fatty acids and steroids
TRINITY_DN21247_c1_g1	*TTC8*	−1.16	Primary ciliogenesis
TRINITY_DN9646_c0_g1	*ZNF764*	−1.55	Regulation of steroid hormone receptors
TRINITY_DN13511_c1_g1	*NSMCE2*	2.33	Response to DNA damage
TRINITY_DN461400_c0_g1	*ATRIP*	−4.21	Response to DNA damage
BPS-EPI vs. control			
TRINITY_DN13603_c1_g3	*NQO1*	−1.28	Antioxidant function
TRINITY_DN3395_c0_g2	*ATG7*	−2.14	Autophagy
TRINITY_DN1211_c0_g1	*ACAA1*	−1.02	Fatty acid oxidation
TRINITY_DN4886_c2_g1	*PC*	3.67	Gluconeogenesis
TRINITY_DN1282_c0_g1	*PCK2*	1.03	Gluconeogenesis
TRINITY_DN51175_c0_g2	*FBP2*	1.74	Glycogen synthesis
TRINITY_DN28922_c0_g4	*SACS*	2.93	Heat shock protein co-chaperoning
TRINITY_DN27431_c0_g1	*DNAJB12*	−2.37	Heat shock protein co-chaperoning
TRINITY_DN1366_c1_g1	*IL1B*	3.61	Immune response and inflammation
TRINITY_DN19710_c0_g1	*CD44*	2.74	Immune response and inflammation
TRINITY_DN214795_c0_g1	*TRDV3*	2.33	Immune response and inflammation
TRINITY_DN476_c1_g1	*CRLF1*	2.20	Immune response and inflammation
TRINITY_DN19459_c0_g3	*CXCL11*	−1.38	Immune response and inflammation
TRINITY_DN13880_c1_g1	*IRF1*	−1.58	Immune response and inflammation
TRINITY_DN8664_c0_g3	*NFATC2*	−2.42	Immune response and inflammation
TRINITY_DN19911_c0_g1	*CEP290*	−1.15	Primary ciliogenesis
TRINITY_DN3174_c0_g2	*CCDC32*	−1.39	Primary ciliogenesis
TRINITY_DN18941_c0_g1	*DPCD*	−4.81	Primary ciliogenesis
TRINITY_DN13272_c0_g1	*CDKL4*	1.26	Regulation of cell cycle
TRINITY_DN1658_c4_g2	*CCND1*	1.17	Regulation of cell cycle
TRINITY_DN9639_c0_g2	*CCNP*	1.10	Regulation of cell cycle
TRINITY_DN25387_c0_g1	*FBXO31*	4.08	Response to DNA damage
TRINITY_DN66484_c0_g1	*PPP4R2*	2.74	Response to DNA damage
TRINITY_DN2236_c0_g1	*XPA*	−1.02	Response to DNA damage
TRINITY_DN10558_c5_g1	*ERCC6L2*	−1.38	Response to DNA damage
TRINITY_DN15667_c0_g1	*UBAP2*	−1.76	Response to DNA damage
TRINITY_DN41770_c4_g1	*CRELD2*	1.06	Unfolded protein response
TRINITY_DN2190_c3_g1	*CTNND2*	1.41	Wnt signaling pathway
TRINITY_DN2408_c0_g1	*LEF1*	1.02	Wnt signaling pathway
TRINITY_DN37095_c0_g1	*TCF4*	−1.70	Wnt signaling pathway

Putative functions of proteins encoded by differentially expressed genes were obtained from UniProt. The complete differentially expressed gene lists are in Supplemental File S1. $n = 3$ pups; relative to control. BPA, bisphenol A; BPS, bisphenol S; CORT, cortisol; EPI, epinephrine.

catecholamine exposure in marine mammals, such as impaired endogenous glucose production and sex hormone synthesis, which are necessary for fasting and reproduction (65). However, EPI-induced upregulation of *PPARGC1A* (PGC1A), which stimulates mitochondrial biogenesis and adipocyte browning in white adipose tissue (66), suggests some adaptive responses to catecholamines in blubber. *PCK1* (PEPCK) is involved in glyceroneogenesis, which is necessary for reesterification of fatty acids released by lipolysis (9), while *PDK4* is a marker of a shift from glucose to fatty acid oxidation (67). Upregulation of *PCK1* and *PDK4* in blubber may serve as an indicator of increased lipid catabolism in response to EPI. EPI and CORT had synergistic effects on expression of *PPARGC1A*, *ADRB2*, *SIK2*, and *PCK1* in PCATS, suggesting that their combination may substantially alter metabolic homeostasis. Together, these results suggest that EPI transcriptionally regulates the adrenergic signaling pathway and its targets in marine mammal blubber, which may lead to altered sensitivity to catecholamines and increases in energy expenditure and lipid and glucose catabolism during stress.

Neuroendocrine signaling.

EPI treatment altered expression of genes encoding receptors for hormones, neurotransmitters, and other signaling molecules, as well as components and targets of their signaling pathways in blubber. These included receptors for acetylcholine, bradykinin, endothelin, estrogen, hydroxycarboxylic acid, retinoic acid, retinol-binding protein 4 (RBP4), serotonin, somatostatin, substance P, and tumor necrosis factor α (TNFA), which were upregulated by EPI and/or CORT-EPI, and receptors for arginine vasopressin, atrial natriuretic peptide, glutamate, growth hormone, leukotrienes, and parathyroid hormone, which were downregulated. Other DEGs were associated with the regulation

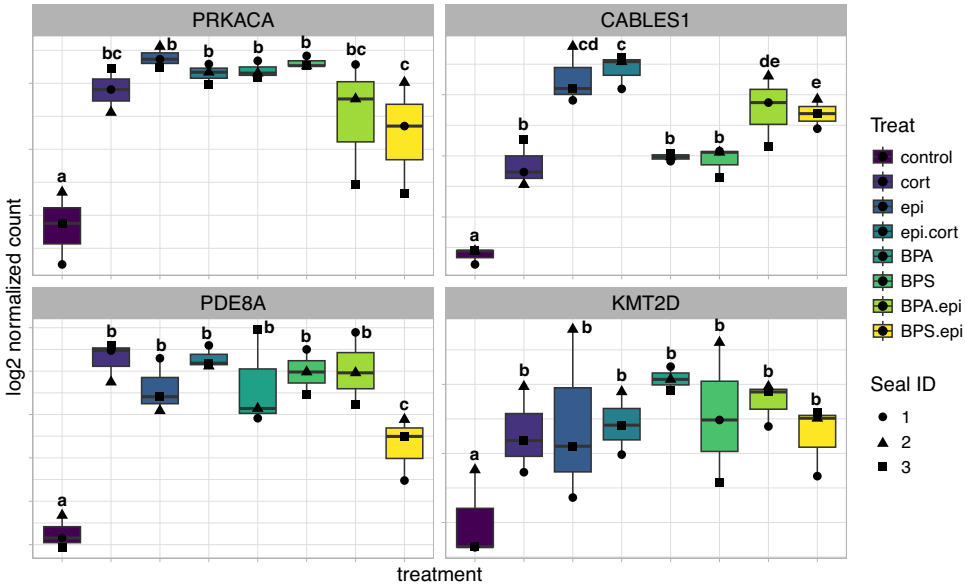

Figure 9. Boxplots showing trimmed mean of *M* values (TMM)-normalized and log2-transformed counts of 4 genes that were differentially expressed in response to hormone and bisphenol treatments in elephant seal precision-cut adipose tissue slices (PCATS). Different letters above the boxes denote gene counts that were significantly different between treatments [linear mixed-effects model (LMM) followed by post hoc tests, $P < 0.1$]. Different colors denote PCATS treatments, whereas different symbol shapes denote individual seals from which PCATS were obtained.

of receptor sensitivity to steroid hormones, steroid biosynthesis, and catabolism of neurotransmitters. EPI also downregulated the gene encoding leptin adipokine (*LEP*), which regulates appetite, lipolysis, and adipocyte browning (68). *LEP* was upregulated by CORT but downregulated by EPI and CORT-EPI in PCATS, suggesting that EPI impairs the blubber response to CORT at the level of *LEP* transcription. The signaling pathways and target genes regulated by these signaling molecules and receptors are involved in angiogenesis, smooth muscle function, inflammation, cell proliferation, blood pressure control, neural signaling, and metabolism, among many other diverse functions, suggesting that catecholamines may alter tissue sensitivity and responsiveness to an array of neuroendocrine signals, with potentially wide-ranging effects on physiology.

Lipid catabolism.

Catecholamines rapidly stimulate lipolysis in adipose tissue primarily via posttranslational mechanisms. The downstream

Table 6. *Genes identified as synergistically regulated (log2 fold change > 1) or antagonistically regulated (log2 fold change < 1) by CORT and EPI, BPA and EPI, or BPS and EPI in precision-cut adipose tissue slices from weaned northern elephant seal pups*

Transcript ID	Gene Symbol	log2 Fold Change	Putative Function
CORT × EPI interaction			
TRINITY_DN63918_c0_g4	*GAK*	5.85	Endocytosis
TRINITY_DN14507_c0_g1	*ANXA6*	5.51	Intracellular calcium storage
TRINITY_DN4873_c0_g2	*TLE6*	3.53	Negative regulation of Wnt signaling
TRINITY_DN20634_c0_g2	*PCID2*	2.98	Immune function
TRINITY_DN331_c1_g2	*RGS3*	1.33	Negative regulation of GPCR signaling
TRINITY_DN5084_c0_g1	*PCK1*	1.30	Glyceroneogenesis
TRINITY_DN5084_c0_g2	*PCK1*	1.26	Glyceroneogenesis
TRINITY_DN2508_c0_g1	*ECSCR*	−0.82	Angiogenesis
TRINITY_DN6067_c1_g1	*ANGPT4*	−1.13	Angiogenesis
TRINITY_DN6067_c1_g2	*ANGPT4*	−1.78	Angiogenesis
TRINITY_DN909_c0_g1	*CDO1*	−0.91	Adipogenesis
TRINITY_DN27111_c0_g2	*PTAR1*	−0.96	Posttranslational modification
TRINITY_DN8779_c0_g1	*EZHIP*	−1.13	Epigenetic regulation
TRINITY_DN16936_c0_g2	*CDH13*	−1.61	Cell–cell adhesion
TRINITY_DN27650_c0_g1	*DTWD1*	−2.33	tRNA processing
TRINITY_DN4417_c9_g1	*SMIM12*	−2.64	Unknown
TRINITY_DN27679_c0_g1	*EDAR*	−2.86	NF-κB signaling
BPA × EPI interaction			
TRINITY_DN10020_c3_g1	*HNRNPM*	4.67	mRNA processing
TRINITY_DN378_c2_g1	*CXCL14*	−5.57	Immune function
BPS × EPI interaction			
TRINITY_DN3384_c4_g1	*RBM6*	3.91	mRNA processing
TRINITY_DN2341_c1_g1	*COQ4*	−0.89	Ubiquinone biosynthesis
TRINITY_DN5581_c0_g1	*NAXE*	−1.59	NAD(P)H damage repair
TRINITY_DN10558_c5_g1	*ERCC6L2*	−2.07	Response to DNA damage

Putative functions of proteins encoded by differentially expressed genes were obtained from UniProt. The complete differentially expressed gene lists are in Supplementary File S3. $n = 3$ pups. BPA, bisphenol A; BPS, bisphenol S; CORT, cortisol; EPI, epinephrine; GPCR, protein-coupled receptor.

mediator CREB also alters expression of genes associated with lipid catabolism (12). Accordingly, expression of a number of DEGs associated with lipolysis and fatty acid oxidation was altered by EPI treatment in NES PCATS, highlighting the transcriptional regulation of lipid catabolism by catecholamines. Lipolysis-associated DEGs that were upregulated in response to EPI encoded intracellular lipase ATGL (*PNPLA2*) and its inhibitor G0S2, lipid droplet proteins, glycerol-transporting aquaporins, fatty acid-binding protein FABP4, lipid uptake inhibitor ANGPTL4, and the lipolysis-stimulating adipokine AZGP1. In contrast, genes associated with lipid uptake, synthesis, and storage (*LPL* and *FASN*) were downregulated in response to EPI. Other EPI-upregulated genes associated with fatty acid oxidation included those encoding beta-oxidation enzymes, a mitochondrial fatty acid transporter, and PPARG coactivators, while the PPARG corepressor *ASXL1* was downregulated. We observed clear interactions between hormones on expression of lipid metabolism genes: *PNPLA2*, *FABP4*, *LPL*, *FASN*, and *PPARA* were differentially expressed only in response to CORT-EPI treatment, but not either hormone alone. Again, the gene expression signature suggests a significant shift toward lipid mobilization and oxidation in response to stress hormones, with significant implications for fasting-adapted marine mammals.

Other functions.

EPI treatment impacted expression of genes with myriad other functions that may have profound impacts on marine mammal blubber physiology. These included genes associated with inflammation, protein ubiquitination and degradation, antioxidant function, adipogenesis, angiogenesis, neurogenesis, cell cycle, apoptosis, ion transport, cytoskeleton and ECM structure and function, and regulation of gene transcription, including epigenetic modification. Some DEGs associated with a particular function (e.g., inflammation) were upregulated, whereas others were downregulated, suggesting that these functions may be fine-tuned in complex and context-dependent ways during stress responses. These findings demonstrate that catecholamines significantly alter the transcriptional landscape of blubber tissue, with potential functional impacts on cell and protein turnover and tissue, redox, and immune homeostasis. Altered expression of transcriptional and epigenetic regulators in response to EPI may have extensive and prolonged impacts on blubber function, lasting long beyond the half-life of catecholamines.

Blubber Response to Bisphenols

Studies in humans and rodents have shown that bisphenols may induce DNA damage and mitochondrial dysfunction, alter redox homeostasis, reduce insulin sensitivity and lipolysis, and have dose- and context-dependent effects on adipogenesis and adipokine production (26, 69). In this study, we found that bisphenol treatments alone had a weak impact on the NES blubber transcriptome compared with stress hormones. However, the combination of EPI with BPA or BPS significantly altered the expression of genes associated with inflammation; cell stress; DNA damage; regulation of Wnt, BMP, and β-adrenergic signaling pathways; nuclear hormone receptor activity; cell cycle; mitochondrial function; primary ciliogenesis; and glucose and lipid metabolism in PCATS. BPA and BPS altered the expression of primarily distinct sets of genes in blubber, as has been shown in mouse adipocytes (70), and affected the transcriptional response of blubber to EPI.

Genes that were responsive solely to bisphenols included the chemokine *CXCL14* and mTOR inhibitor *DDIT4L*, which were upregulated only in response to BPA, mitochondrial damage response gene *PGAM5*, which was downregulated only in response to BPS, and selenium-responsive gene *SELENOV*, which was downregulated in response to both BPS and BPA. The addition of EPI with BPA and BPS attenuated the effects of bisphenols on the expression of these markers in blubber. *CXCL14* regulates insulin sensitivity, adipocyte browning, and adipocyte-to-macrophage communication (71, 72), whereas *DDIT4L* promotes autophagy in response to cell stress (73). Their upregulation in PCATS in response to BPA suggests that bisphenols may alter immune and metabolic function in blubber. *PGAM5* induces mitochondrial biogenesis, fission, mitophagy, and/or cell death, depending on the severity of damage to this organelle (74). Its downregulation in response to BPS suggests reduced sensitivity to mitochondrial damage, which could impair mitochondrial health, and thus metabolic and redox homeostasis, in marine mammals. *SELENOV* stimulates lipolysis and increases energy expenditure (75); its downregulation in PCATS in response to bisphenols is consistent with their obesogenic effects reported in other species (26). Together, changes in expression of these markers suggest that bisphenols may have complex effects on cellular homeostasis by altering responses to cell stress, insulin sensitivity, and lipid metabolism in blubber, and have implications for the ability of marine mammals with high bisphenol loads to mobilize fat stores to support energetically demanding life-history stages.

BPA and BPS treatments alone affected the expression of genes that were also regulated by CORT and EPI, suggesting that bisphenols may target similar pathways to those regulated by stress hormones in blubber. Although BPA has been shown to bind GR in biomedical model systems (76), it is unknown whether bisphenols interact with β-adrenergic receptor or any downstream components of its signaling pathway. BPA and EPI showed potential antagonistic effects on expression of *SPP1*, which encodes osteopontin, a proinflammatory cytokine associated with insulin resistance and inhibition of adipogenesis (77), suggesting that BPA may reduce immune and metabolic responses to catecholamines. BPS and EPI showed a potential antagonistic effect on the gene encoding rhodopsin, which was downregulated in response to both treatments alone and in combination. Although *RHO* is mainly involved in phototransduction in the retina, it is also expressed in extraocular tissues such as adipose (78), and it may regulate *ADRB3* expression and lipolysis (79). Therefore, the inhibitory effect of EPI and BPS on *RHO* expression in PCATS may be mediated, in part, via adrenergic receptors. However, the functional consequences of this effect are impossible to predict as the function of rhodopsin in adipose tissue in vivo is presently unknown.

Finally, we identified suites of genes that were differentially expressed only in response to the combination of bisphenol-EPI treatments, but not EPI, CORT, or EPI-CORT, suggesting interactive effects of catecholamines and bisphenols on their expression. These included inflammation

regulators *IKBKB* and *IL1B*, antioxidant enzyme *NQO1*, autophagy and adipogenesis regulator *ATG7*, DNA repair enzymes, cell cycle regulators, β-oxidation enzymes, and many others. The functions of these genes were consistent with reported effects of bisphenols (i.e., DNA damage, oxidative stress, cell proliferation, modulation of the immune system, and obesity) in other systems (27). Interestingly, the most highly downregulated genes by BPA-EPI and BPS-EPI were associated with primary cilia, which are organelles that organize signal transduction pathways and play a role in adipogenesis (80). Most importantly, we found evidence of a potential synergistic interaction of bisphenols and EPI on the expression of RNA-modifying enzymes and antagonistic interactions on the expression of genes associated with responses to metabolite and DNA damage. These data suggest that bisphenols and EPI may interact to dysregulate adipocyte proliferation and differentiation in blubber, and that the combination of catecholamines and bisphenols may impact DNA and RNA stability, redox homeostasis, and inflammation. Therefore, marine mammals with high levels of bisphenol exposure may be especially sensitive to the physiological effects of stress hormones. Stressed marine mammals, in turn, may be more vulnerable to the cytotoxic effects of contaminants.

Perspectives and Significance

Our study demonstrates the utility of ex vivo systems such as PCATS for combinatorial and functional experiments in marine mammals. Using this system, we identified blubber genes that were regulated by cortisol, epinephrine, BPA, and BPS individually and in combination, providing novel markers of stress responses and contaminant exposure and hypotheses on their downstream effects on marine mammal physiology. To our knowledge, this is the first study to examine the marine mammal blubber transcriptome response to direct stimulation with catecholamines and bisphenols. We suggest that catecholamines may have long-lasting and wide-ranging effects on blubber tissue (e.g., altered sensitivity to a variety of neuroendocrine signals and epigenetic regulation of gene expression), especially in combination with GCs and bisphenols, and should, therefore, be considered when evaluating the effects of stress on wildlife. Bisphenols, in turn, may alter blubber responses to lipid-mobilizing hormone signals and may impact DNA and mitochondrial stability, redox homeostasis, steroid hormone biosynthesis, energy expenditure, immune responses, and other functions, which have significant implications for marine mammal health and survival. Although the study was limited by a small sample size, one age class of animals, and single doses of hormones and contaminants, it provides a framework for further multistressor studies, which should examine the impacts of varying concentrations of contaminants on blubber responses to other stress-responsive hormones in marine mammals, such as cortisol, aldosterone, and thyroid hormone.

DATA AVAILABILITY

Raw RNAseq data is available at NCBI SRA, Accession No.: PRJNA989379. Transcriptome assembly and annotation files are available at https://doi.org/10.6084/m9.figshare.21804192.

SUPPLEMENTAL DATA

Supplemental Files S1–S3 and Fig. S1: https://doi.org/10.6084/m9.figshare.23612637.v3.

ACKNOWLEDGMENTS

The authors are grateful to D. Costa, P. Robinson, and Año Nuevo Reserve for facilitating access to the animals, to D. Smith for access to the tissue culture laboratory, and to M. Martin for advice on statistical analyses.

GRANTS

This work was funded by a Fonds de la Recherche Scientifique (Belgium) grant to L. Pirard and C. Debier (Research Credit No. 33684148) and University of the Pacific College Research Fund grant to J. Khudyakov.

DISCLOSURES

No conflicts of interest, financial or otherwise, are declared by the authors.

AUTHOR CONTRIBUTIONS

L.P., C.D., and J.K. conceived and designed research; L.K., L.P., C.D., and D.C. performed experiments; L.K. and J.K. analyzed data; L.K., L.P., C.D., D.C., and J.K. interpreted results of experiments; L.K. and J.K. prepared figures; L.K. and J.K. drafted manuscript; L.K., L.P., C.D., D.C., and J.K. edited and revised manuscript; L.K., L.P., C.D., D.C., and J.K. approved final version of manuscript.

REFERENCES

1. **O'Hara CC**, **Frazier M**, **Halpern BS.** At-risk marine biodiversity faces extensive, expanding, and intensifying human impacts. *Science* 372: 84–87, 2021. doi:10.1126/science.abe6731.
2. **Halpern BS**, **Frazier M**, **Potapenko J**, **Casey KS**, **Koenig K**, **Longo C**, **Lowndes JS**, **Rockwood RC**, **Selig ER**, **Selkoe KA**, **Walbridge S.** Spatial and temporal changes in cumulative human impacts on the world's ocean. *Nat Commun* 6: 7615, 2015. doi:10.1038/ncomms8615.
3. **Nelms SE**, **Alfaro-Shigueto J**, **Arnould JPY**, **Avila IC**, **Bengtson Nash S**, **Campbell E**, **et al.** Marine mammal conservation: over the horizon. *Endang Species Res* 44: 291–325, 2021. doi:10.3354/esr01115.
4. **Gormally BMG**, **Romero LM.** What are you actually measuring? A review of techniques that integrate the stress response on distinct timescales. *Funct Ecol* 34: 2030–2044, 2020. doi:10.1111/1365-2435.13648.
5. **Kuti D**, **Winkler Z**, **Horváth K**, **Juhász B**, **Szilvásy-Szabó A**, **Fekete C**, **Ferenczi S**, **Kovács KJ.** The metabolic stress response: adaptation to acute-, repeated- and chronic challenges in mice. *iScience* 25: 104693, 2022. doi:10.1016/j.isci.2022.104693.
6. **Hing S**, **Narayan EJ**, **Thompson RCA**, **Godfrey SS.** The relationship between physiological stress and wildlife disease: consequences for health and conservation. *Wildl Res* 43: 51–60, 2016. doi:10.1071/WR15183.
7. **Wada H.** Damage-fitness model: the missing piece in integrative stress models. *Stress* 22: 548–562, 2019. doi:10.1080/10253890.2019.1614556.
8. **Sokolova IM.** Energy-limited tolerance to stress as a conceptual framework to integrate the effects of multiple stressors. *Integr Comp Biol* 53: 597–608, 2013. doi:10.1093/icb/ict028.
9. **Kersten S.** The impact of fasting on adipose tissue metabolism. *Biochim Biophys Acta Mol Cell Biol Lipids* 1868: 159262, 2023. doi:10.1016/j.bbalip.2022.159262.
10. **Peckett AJ**, **Wright DC**, **Riddell MC.** The effects of glucocorticoids on adipose tissue lipid metabolism. *Metabolism* 60: 1500–1510, 2011. doi:10.1016/j.metabol.2011.06.012.

11. **Altarejos JY**, **Montminy M.** CREB and the CRTC co-activators: sensors for hormonal and metabolic signals. *Nat Rev Mol Cell Biol* 12: 141–151, 2011. doi:10.1038/nrm3072.
12. **Guilherme A**, **Rowland LA**, **Wang H**, **Czech MP.** The adipocyte supersystem of insulin and cAMP signaling. *Trends Cell Biol* 33: 340–354, 2023. doi:10.1016/j.tcb.2022.07.009.
13. **Lee MJ**, **Pramyothin P**, **Karastergiou K**, **Fried SK.** Deconstructing the roles of glucocorticoids in adipose tissue biology and the development of central obesity. *Biochim Biophys Acta* 1842: 473–481, 2014. doi:10.1016/j.bbadis.2013.05.029.
14. **Mir N**, **Chin SA**, **Riddell MC**, **Beaudry JL.** Genomic and non-genomic actions of glucocorticoids on adipose tissue lipid metabolism. *Int J Mol Sci* 22: 8503, 2021. doi:10.3390/ijms22168503.
15. **Korenfeld N**, **Finkel M**, **Buchshtab N**, **Bar-Shimon M**, **Charni-Natan M**, **Goldstein I.** Fasting hormones synergistically induce amino acid catabolism genes to promote gluconeogenesis. *Cell Mol Gastroenterol Hepatol* 12: 1021–1036, 2021. doi:10.1016/j.jcmgh.2021.04.017.
16. **Goldberg D**, **Charni-Natan M**, **Buchshtab N**, **Bar-Shimon M**, **Goldstein I.** Hormone-controlled cooperative binding of transcription factors drives synergistic induction of fasting-regulated genes. *Nucleic Acids Res* 50: 5528–5544, 2022. doi:10.1093/nar/gkac358.
17. **Hill MJ**, **Suzuki S**, **Segars JH**, **Kino T.** CRTC2 is a coactivator of GR and couples GR and CREB in the regulation of hepatic gluconeogenesis. *Mol Endocrinol* 30: 104–117, 2016. doi:10.1210/me.2015-1237.
18. **Champagne CD**, **Houser DS**, **Costa DP**, **Crocker DE.** The effects of handling and anesthetic agents on the stress response and carbohydrate metabolism in northern elephant seals. *PLoS One* 7: e38442, 2012. doi:10.1371/journal.pone.0038442.
19. **Deyarmin JS**, **McCormley MC**, **Champagne CD**, **Stephan AP**, **Pujade Busqueta L**, **Crocker DE**, **Houser DS**, **Khudyakov JI.** Blubber transcriptome responses to repeated ACTH administration in a marine mammal. *Sci Rep* 9: 2718, 2019. doi:10.1038/s41598-019-39089-2.
20. **Khudyakov JI**, **Champagne CD**, **Meneghetti LM**, **Crocker DE.** Blubber transcriptome response to acute stress axis activation involves transient changes in adipogenesis and lipolysis in a fasting-adapted marine mammal. *Sci Rep* 7: 42110, 2017. doi:10.1038/srep42110.
21. **Pirotta E**, **Thomas L**, **Costa DP**, **Hall AJ**, **Harris CM**, **Harwood J**, **Kraus SD**, **Miller PJO**, **Moore MJ**, **Photopoulou T**, **Rolland RM**, **Schwacke L**, **Simmons SE**, **Southall BL**, **Tyack PL.** Understanding the combined effects of multiple stressors: a new perspective on a longstanding challenge. *Sci Total Environ* 821: 153322, 2022. doi:10.1016/j.scitotenv.2022.153322.
22. **Jasrotia R**, **Langer S**, **Dhar M.** Endocrine disrupting chemicals in aquatic ecosystems: an emerging threat to wildlife and human health. *Proc Zool Soc* 74: 634–647, 2021. doi:10.1007/s12595-021-00410-5.
23. **Page-Karjian A**, **Lo CF**, **Ritchie B**, **Harms CA**, **Rotstein DS**, **Han S**, **Hassan SM**, **Lehner AF**, **Buchweitz JP**, **Thayer VG**, **Sullivan JM**, **Christiansen EF**, **Perrault JR.** Anthropogenic contaminants and histopathological findings in stranded cetaceans in the southeastern United States, 2012–2018. *Front Mar Sci* 7: 630, 2020. doi:10.3389/fmars.2020.00630.
24. **Guo Y**, **Shi W**, **Liu Z**, **Sun X**, **Wu J**, **Wu Y.** Bisphenol A alternatives continuously contribute to the endocrine disruption in cetaceans. *Environ Int* 171: 107679, 2023. doi:10.1016/j.envint.2022.107679.
25. **MacKay H**, **Abizaid A.** A plurality of molecular targets: the receptor ecosystem for bisphenol-A (BPA). *Horm Behav* 101: 59–67, 2018. doi:10.1016/j.yhbeh.2017.11.001.
26. **Ahmed F**, **Pereira MJ**, **Aguer C.** Bisphenols and the development of type 2 diabetes: the role of the skeletal muscle and adipose tissue. *Environments* 8: 35, 2021. doi:10.3390/environments8040035.
27. **Qiu W**, **Zhan H**, **Hu J**, **Zhang T**, **Xu H**, **Wong M**, **Xu B**, **Zheng C.** The occurrence, potential toxicity, and toxicity mechanism of bisphenol S, a substitute of bisphenol A: a critical review of recent progress. *Ecotoxicol Environ Saf* 173: 192–202, 2019. doi:10.1016/j.ecoenv.2019.01.114.
28. **Gassel M**, **Rochman CM.** The complex issue of chemicals and microplastic pollution: a case study in North Pacific lanternfish. *Environ Pollut* 248: 1000–1009, 2019. doi:10.1016/j.envpol.2019.03.002.
29. **Goetsch C**, **Conners MG**, **Budge SM**, **Mitani Y**, **Walker WA**, **Bromaghin JF**, **Simmons SE**, **Reichmuth C**, **Costa DP.** Energy-rich mesopelagic fishes revealed as a critical prey resource for a deep-diving predator using quantitative fatty acid signature analysis. *Front Mar Sci* 5: 430, 2018. doi:10.3389/fmars.2018.00430.
30. **Adachi T**, **Takahashi A**, **Costa DP**, **Robinson PW**, **Hückstädt LA**, **Peterson SH**, **Holser RR**, **Beltran RS**, **Keates TR**, **Naito Y.** Forced into an ecological corner: round-the-clock deep foraging on small prey by elephant seals. *Sci Advances* 7: eabg3628, 2021. doi:10.1126/sciadv.abg3628.
31. **Debier C**, **Pirard L**, **Verhaegen M**, **Rzucidlo C**, **Tinant G**, **Dewulf C**, **Larondelle Y**, **Smith DR**, **Rees J-F**, **Crocker DE.** In vitro lipolysis and leptin production of elephant seal blubber using precision-cut adipose tissue slices. *Front Physiol* 11: 615784, 2020. doi:10.3389/fphys.2020.615784.
32. **Nehring I**, **Falkowska L**, **Staniszewska M**, **Pawliczka I**, **Bodziach K.** Maternal transfer of phenol derivatives in the Baltic grey seal *Halichoerus grypus*. *Environ Pollut* 242: 1642–1651, 2018. doi:10.1016/j.envpol.2018.07.113.
33. **Héliès-Toussaint C**, **Peyre L**, **Costanzo C**, **Chagnon M-C**, **Rahmani R.** Is bisphenol S a safe substitute for bisphenol A in terms of metabolic function? An in vitro study. *Toxicol Appl Pharmacol* 280: 224–235, 2014. doi:10.1016/j.taap.2014.07.025.
34. **Towns J**, **Cockerill T**, **Dahan M**, **Foster I**, **Gaither K**, **Grimshaw A**, **Hazlewood V**, **Lathrop S**, **Lifka D**, **Peterson GD**, **Roskies R**, **Scott JR**, **Wilkins-Diehr N.** XSEDE: accelerating scientific discovery. *Comput Sci Eng* 16: 62–74, 2014. doi:10.1109/MCSE.2014.80.
35. **Haas BJ**, **Papanicolaou A**, **Yassour M**, **Grabherr M**, **Blood PD**, **Bowden J**, **Couger MB**, **Eccles D**, **Li B**, **Lieber M**, **MacManes MD**, **Ott M**, **Orvis J**, **Pochet N**, **Strozzi F**, **Weeks N**, **Westerman R**, **William T**, **Dewey CN**, **Henschel R**, **LeDuc RD**, **Friedman N**, **Regev A.** De novo transcript sequence reconstruction from RNA-seq using the Trinity platform for reference generation and analysis. *Nat Protoc* 8: 1494–1512, 2013. doi:10.1038/nprot.2013.084.
36. **Manni M**, **Berkeley MR**, **Seppey M**, **Simão FA**, **Zdobnov EM.** BUSCO update: novel and streamlined workflows along with broader and deeper phylogenetic coverage for scoring of eukaryotic, prokaryotic, and viral genomes. *Mol Biol Evol* 38: 4647–4654, 2021. doi:10.1093/molbev/msab199.
37. **Buchfink B**, **Reuter K**, **Drost H-G.** Sensitive protein alignments at tree-of-life scale using DIAMOND. *Nat Methods* 18: 366–368, 2021. doi:10.1038/s41592-021-01101-x.
38. **Bray NL**, **Pimentel H**, **Melsted P**, **Pachter L.** Near-optimal probabilistic RNA-seq quantification. *Nat Biotechnol* 34: 525–527, 2016 [Erratum in *Nat Biotechnol* 34: 888, 2016]. doi:10.1038/nbt.3519.
39. **R Core Team.** R: A Language and Environment for Statistical Computing. Vienna, Austria: R Foundation for Statistical Computing, 2019. https://www.R-project.org.
40. **Love MI**, **Huber W**, **Anders S.** Moderated estimation of fold change and dispersion for RNA-seq data with DESeq2. *Genome Biol* 15: 550, 2014. doi:10.1186/s13059-014-0550-8.
41. **Law C**, **Zeglinski K**, **Dong X**, **Alhamdoosh M**, **Smyth G**, **Ritchie M.** A guide to creating design matrices for gene expression experiments. *F1000Res* 9: 1444, 2020. doi:10.12688/f1000research.27893.1.
42. **Conway JR**, **Lex A**, **Gehlenborg N.** UpSetR: an R package for the visualization of intersecting sets and their properties. *Bioinformatics* 33: 2938–2940, 2017. doi:10.1093/bioinformatics/btx364.
43. **Wu T**, **Hu E**, **Xu S**, **Chen M**, **Guo P**, **Dai Z**, **Feng T**, **Zhou L**, **Tang W**, **Zhan L**, **Fu X**, **Liu S**, **Bo X**, **Yu G.** clusterProfiler 4.0: a universal enrichment tool for interpreting omics data. *Innovation (Camb)* 2: 100141, 2021. doi:10.1016/j.xinn.2021.100141.
44. **Kuznetsova A**, **Brockhoff PB**, **Christensen RHB.** lmerTest package: tests in linear mixed effects models. *J Stat Soft* 82: 1–26, 2017. doi:10.18637/jss.v082.i13.
45. **Searle SR**, **Speed FM**, **Milliken GA.** Population marginal means in the linear model: an alternative to least squares means. *Am Stat* 34: 216–221, 1980.doi:10.2307/2684063.
46. **Higareda-Almaraz JC**, **Karbiener M**, **Giroud M**, **Pauler FM**, **Gerhalter T**, **Herzig S**, **Scheideler M.** Norepinephrine triggers an immediate-early regulatory network response in primary human white adipocytes. *BMC Genomics* 19: 794, 2018. doi:10.1186/s12864-018-5173-0.
47. **St. Laurent G**, **Shtokalo D**, **Tackett MR**, **Yang Z**, **Vyatkin Y**, **Milos PM**, **Seilheimer B**, **McCaffrey TA**, **Kapranov P.** On the importance of small changes in RNA expression. *Methods* 63: 18–24, 2013. doi:10.1016/j.ymeth.2013.03.027.
48. **London E**, **Stratakis CA.** The regulation of PKA signaling in obesity and in the maintenance of metabolic health. *Pharmacol Ther* 237: 108113, 2022. doi:10.1016/j.pharmthera.2022.108113.

49. **Deyarmin J**, **Hekman R**, **Champagne C**, **McCormley M**, **Stephan A**, **Crocker D**, **Houser D**, **Khudyakov J.** Blubber proteome response to repeated ACTH administration in a wild marine mammal. *Comp Biochem Physiol Part D Genomics Proteomics* 33: 100644, 2020. doi:10.1016/j.cbd.2019.100644.
50. **Fang R**, **Yang S**, **Gu X**, **Li C**, **Bi N**, **Wang H-L.** Early-life exposure to bisphenol A induces dysregulation of lipid homeostasis by the upregulation of SCD1 in male mice. *Environ Pollut* 304: 119201, 2022. doi:10.1016/j.envpol.2022.119201.
51. **Epstein PM**, **Basole C**, **Brocke S.** The role of PDE8 in T cell recruitment and function in inflammation. *Front Cell Dev Biol* 9: 636778, 2021. doi:10.3389/fcell.2021.636778.
52. **Dhar SS**, **Lee MG.** Cancer-epigenetic function of the histone methyltransferase KMT2D and therapeutic opportunities for the treatment of KMT2D-deficient tumors. *Oncotarget* 12: 1296–1308, 2021. doi:10.18632/oncotarget.27988.
53. **Jia-Rong H**, **Guang-Mou T**, **Yong L**, **Zhi S.** the emerging role of cables1 in cancer and other diseases. *Mol Pharmacol* 92: 240–245, 2017 [Erratum in *Mol Pharmacol* 92: 629, 2017]. doi:10.1124/mol.116.107730.
54. **Rahbani JF**, **Scholtes C**, **Lagarde DM**, **Hussain MF**, **Roesler A**, **Dykstra CB**, **Bunk J**, **Samborska B**, **O'Brien SL**, **Tripp E**, **Pacis A**, **Angueira AR**, **Johansen OS**, **Cinkornpumin J**, **Hossain I**, **Lynes MD**, **Zhang Y**, **White AP**, **Pastor WA**, **Chondronikola M**, **Sidossis L**, **Klein S**, **Kralli A**, **Cypess AM**, **Pedersen SB**, **Jessen N**, **Tseng YH**, **Gerhart-Hines Z**, **Seale P**, **Calebiro D**, **Giguère V**, **Kazak L.** ADRA1A–Gαq signalling potentiates adipocyte thermogenesis through CKB and TNAP. *Nat Metab* 4: 1459–1473, 2022. doi:10.1038/s42255-022-00667-w.
55. **Ronchetti S**, **Migliorati G**, **Riccardi C.** GILZ as a mediator of the anti-inflammatory effects of glucocorticoids. *Front Endocrinol (Lausanne)* 6: 170, 2015. doi:10.3389/fendo.2015.00170.
56. **Ahonen MA**, **Höring M**, **Nguyen VD**, **Qadri S**, **Taskinen JH**, **Nagaraj M**, **Wabitsch M**, **Fischer-Posovszky P**, **Zhou Y**, **Liebisch G**, **Haridas PAN**, **Yki-Järvinen H**, **Olkkonen VM.** Insulin-inducible THRSP maintains mitochondrial function and regulates sphingolipid metabolism in human adipocytes. *Mol Med* 28: 68, 2022. doi:10.1186/s10020-022-00496-3.
57. **Ravindranathan P**, **Lange CA**, **Raj GV.** Minireview: deciphering the cellular functions of PELP1. *Mol Endocrinol* 29: 1222–1229, 2015. doi:10.1210/me.2015-1049.
58. **Han SO**, **Kommaddi RP**, **Shenoy SK.** Distinct roles for β-arrestin2 and arrestin-domain-containing proteins in β2 adrenergic receptor trafficking. *EMBO Rep* 14: 164–171, 2013. doi:10.1038/embor.2012.187.
59. **Guo Y-Y**, **Li B-Y**, **Xiao G**, **Liu Y**, **Guo L**, **Tang Q-Q.** Cdo1 promotes PPARγ-mediated adipose tissue lipolysis in male mice. *Nat Metab* 4: 1352–1368, 2022. doi:10.1038/s42255-022-00644-3.
60. **Onder Y**, **Green CB.** Rhythms of metabolism in adipose tissue and mitochondria. *Neurobiol Sleep Circadian Rhythms* 4: 57–63, 2018. doi:10.1016/j.nbscr.2018.01.001.
61. **McCormley MC**, **Champagne CD**, **Deyarmin JS**, **Stephan AP**, **Crocker DE**, **Houser DS**, **Khudyakov JI.** Repeated adrenocorticotropic hormone administration alters adrenal and thyroid hormones in free-ranging elephant seals. *Conserv Physiol* 6: coy040, 2018. doi:10.1093/conphys/coy040.
62. **Kineman RD**, **del Rio-Moreno M**, **Sarmento-Cabral A.** 40 YEARS of IGF1: Understanding the tissue-specific roles of IGF1/IGF1R in regulating metabolism using the Cre/loxP system. *J Mol Endocrinol* 61: T187–T198, 2018. doi:10.1530/JME-18-0076.
63. **Sun Z**, **Jiang Q**, **Li J**, **Guo J.** The potent roles of salt-inducible kinases (SIKs) in metabolic homeostasis and tumorigenesis. *Signal Transduct Target Ther* 5: 150, 2020. doi:10.1038/s41392-020-00265-w.
64. **Chen L**, **Fan F**, **Wu L**, **Zhao Y.** The nuclear receptor 4A family members: mediators in human disease and autophagy. *Cell Mol Biol Lett* 25: 48, 2020. doi:10.1186/s11658-020-00241-w.
65. **Champagne CD**, **Crocker DE**, **Fowler MA**, **Houser DS.** Fasting physiology of the pinnipeds: the challenges of fasting while maintaining high energy expenditure and nutrient delivery for lactation. In: *Comparative Physiology of Fasting, Starvation, and Food Limitation*, edited by McCue, M. Berlin, Heidelberg, Germany: Springer, 2012, p. 309–336.
66. **Heinonen S**, **Jokinen R**, **Rissanen A**, **Pietiläinen KH.** White adipose tissue mitochondrial metabolism in health and in obesity. *Obes Rev* 21: e12958, 2020. doi:10.1111/obr.12958.
67. **Pettersen IKN**, **Tusubira D**, **Ashrafi H**, **Dyrstad SE**, **Hansen L**, **Liu XZ**, **Nilsson LIH**, **Løvsletten NG**, **Berge K**, **Wergedahl H**, **Bjørndal B**, **Fluge Ø**, **Bruland O**, **Rustan AC**, **Halberg N**, **Røsland GV**, **Berge RK**, **Tronstad KJ.** Upregulated PDK4 expression is a sensitive marker of increased fatty acid oxidation. *Mitochondrion* 49: 97–110, 2019. doi:10.1016/j.mito.2019.07.009.
68. **Caron A**, **Lee S**, **Elmquist JK**, **Gautron L.** Leptin and brain–adipose crosstalks. *Nat Rev Neurosci* 19: 153–165, 2018. doi:10.1038/nrn.2018.7.
69. **Gassman NR.** Induction of oxidative stress by bisphenol A and its pleiotropic effects. *Environ Mol Mutagen* 58: 60–71, 2017. doi:10.1002/em.22072.
70. **Boucher JG**, **Gagné R**, **Rowan-Carroll A**, **Boudreau A**, **Yauk CL**, **Atlas E.** Bisphenol A and bisphenol S induce distinct transcriptional profiles in differentiating human primary preadipocytes. *PLoS One* 11: e0163318, 2016. doi:10.1371/journal.pone.0163318.
71. **Cereijo R**, **Gavaldà-Navarro A**, **Cairó M**, **Quesada-López T**, **Villarroya J**, **Morón-Ros S**, **Sánchez-Infantes D**, **Peyrou M**, **Iglesias R**, **Mampel T**, **Turatsinze JV**, **Eizirik DL**, **Giralt M**, **Villarroya F.** CXCL14, a brown adipokine that mediates brown-fat-to-macrophage communication in thermogenic adaptation. *Cell Metab* 28: 750–763. E6, 2018. doi:10.1016/j.cmet.2018.07.015.
72. **Cereijo R**, **Quesada-López T**, **Gavaldà-Navarro A**, **Tarascó J**, **Pellitero S**, **Reyes M**, **Puig-Domingo M**, **Giralt M**, **Sánchez-Infantes D**, **Villarroya F.** The chemokine CXCL14 is negatively associated with obesity and concomitant type-2 diabetes in humans. *Int J Obes (Lond)* 45: 706–710, 2021. doi:10.1038/s41366-020-00732-y.
73. **Simonson B**, **Subramanya V**, **Chan MC**, **Zhang A**, **Franchino H**, **Ottaviano F**, **Mishra MK**, **Knight AC**, **Hunt D**, **Ghiran I**, **Khurana TS**, **Kontaridis MI**, **Rosenzweig A**, **Das S.** DDIT4L promotes autophagy and inhibits pathological cardiac hypertrophy in response to stress. *Sci Signal* 10: eaaf5967, 2017. doi:10.1126/scisignal.aaf5967.
74. **Liang M-Z**, **Ke T-L**, **Chen L.** Mitochondrial protein PGAM5 emerges as a new regulator in neurological diseases. *Front Mol Neurosci* 14: 730604, 2021. doi:10.3389/fnmol.2021.730604.
75. **Chen LL**, **Huang JQ**, **Wu YY**, **Chen LB**, **Li SP**, **Zhang X**, **Wu S**, **Ren FZ**, **Lei XG.** Loss of Selenov predisposes mice to extra fat accumulation and attenuated energy expenditure. *Redox Biol* 45: 102048, 2021. doi:10.1016/j.redox.2021.102048.
76. **Sargis RM**, **Johnson DN**, **Choudhury RA**, **Brady MJ.** environmental endocrine disruptors promote adipogenesis in the 3T3-L1 cell line through glucocorticoid receptor activation. *Obesity (Silver Spring)* 18: 1283–1288, 2010. doi:10.1038/oby.2009.419.
77. **Moreno-Viedma V**, **Tardelli M**, **Zeyda M**, **Sibilia M**, **Burks JD**, **Stulnig TM.** Osteopontin-deficient progenitor cells display enhanced differentiation to adipocytes. *Obes Res Clin Pract* 12: 277–285, 2018. doi:10.1016/j.orcp.2018.02.006.
78. **Regard JB**, **Sato IT**, **Coughlin SR.** Anatomical profiling of G protein-coupled receptor expression. *Cell* 135: 561–571, 2008. doi:10.1016/j.cell.2008.08.040.
79. **Park PJ**, **Cho JY**, **Cho E-G.** Specific visible radiation facilitates lipolysis in mature 3T3-L1 adipocytes via rhodopsin-dependent β3-adrenergic signaling. *Eur J Cell Biol* 96: 301–311, 2017. doi:10.1016/j.ejcb.2017.03.015.
80. **Hilgendorf KI.** Primary cilia are critical regulators of white adipose tissue expansion. *Front Physiol* 12: 769367, 2021. doi:10.3389/fphys.2021.769367.